5-2020

PRECLINICAL STUDIES OF A NOVEL IDH1 INHIBITOR IN ACUTE MYELOID LEUKEMIA (AML)

Vivian Salama

PRECLINICAL STUDIES OF A NOVEL IDH1 INHIBITOR IN ACUTE MYELOID LEUKEMIA (AML)

Vivian Salama, MD

APPROVED:

Marina Konopleva, MD, PhD
Advisory Committee Chair

Koichi Takahashi, MD

Shiaw-Yih (Phoebus) Lin, PhD

Sean Post, PhD

Florian Muller, PhD

APPROVED:

Dean, The University of Texas
MD Anderson Cancer Center UTHealth Graduate School of Biomedical Sciences

PRECLINICAL STUDIES OF A NOVEL IDH1 INHIBITOR IN ACUTE MYELOID LEUKEMIA (AML)

THESIS

Presented to the Faculty of

The University of Texas

MD Anderson Cancer Center UTHealth

Graduate School of Biomedical Sciences

in Partial Fulfillment

of the Requirements

for the Degree of

MASTER OF SCIENCE

by

Vivian Salama, M.D.

Houston, Texas

May, 2020

Acknowledgments:

Thanks to God for his generous blessings. Without his grace, I would not be able to accomplish that project.

I would like to sincerely thank my amazing mentor Dr. Marina Konopleva, MD. PHD, as without her great support, that work would not have been done. She encouraged me to take my first steps in the scientific field and to get the self confidence that was enough to do a lot of work in a short time. She was very kind, humble and very knowledgeable. Dr. Konopleva is a perfect mentor for any graduate and even undergraduate student. She was a source of my success and my luck at USA, and I owe to her with what I am in now.

I thank all of my committee members: Dr. Koichi Takahashi MD, Dr. Shiaw-Yih Lin PHD, Dr. Sean Post PHD, and Dr. Florian Muller PHD. They were very supportive and available whenever I needed any help, I would like to thank them for the time and effort they spent for development of my project.

I would also like to give special thanks to Dr. Anna Skwarska PHD. She actually was the first one who caught my hands to take my first steps in lab work and doing the scientific experiments, she taught me a lot of the basics of the lab work. Despite the short time we spent together, I had learned many things from her. She is now in a good position at the University of Oxford, England, I wish her a good luck.

I would like to thank all my lab members: Zhihong Zeng, Shelley M Herbrich, Venitha Kuruvilla, Antonio Cavazos, Lina Han, Qi Zhang, Natalia Baran, Tiyanu Cai, Conne, Helen Ma, Kala, Taylor and Karine Harutyunyan. Each of them helped me with something, and supported me in my experiments. Their support was not only physically but also emotionally. They were very nice friends throughout my stay at lab.

Moreover, special thanks to all of the staff of GSBS for their support and their hard work to ensure that each student has the special care and the good environment to learn. Thanks to the Deans of the GSBS; Dr. Michelle Barton and Dr. Michael Blackburn. Thanks to Dr. Eric Swindell and Dr. Kelly Moore for their great work in the master program. I can't forget to thank Dr. Lindsey Minter. Though she left the school but I can't forget her pure heart and her care for all of her students. I wish her a good luck.

Special thanks to Dr. Mien Chie Hung PHD. He served as my mentor through my first year, he was really a very nice and supportive mentor. I am so proud that I gained from his experience even for a short time but it was a very valuable time. He is a role model of a successful mentor.

It is also important to thank the corner stones of my life; my Mother; Laila, My awesome husband Dr. Mina Hanna MD, My parents-in-law; Amal and Fawzi, and my cute kids, John and Sherry. Simply, I could not have done this work without them. They took extra miles to help me and support me to finish my master thesis. They went through hard times with me while I was busy working, studying and taking my exams, with happiness and endurance.

I dedicate this project to the soul of my father who looks at me now from heaven. I say to him; you were always proud of me through whole of my life, you wished to see me a physician and you did, you wished to see me a happy wife and you did and you wished to see me graduated from a big international graduate school and now I do for you. Thank you for your prayers for me.

PRECLINICAL STUDIES OF A NOVEL IDH1 INHIBITOR IN ACUTE MYELOID LEUKEMIA (AML)

Vivian Salama, MD.

Advisory Professor: Marina Konopleva, MD, Ph.D.

Abstract

LY3410738, a novel covalent Isocitrate Dehydrogenase 1 (IDH1) inhibitor in Acute Myeloid Leukemia, it is more effective than Ivosidenib (AG120) and has a potent anti-leukemic effect against IDH1 mutant acute myeloid leukemia in combination with Venetoclax (ABT-199).

Acute myeloid Leukemia (AML) is an aggressive neoplastic blood disorder characterized by proliferation of poorly differentiated cells of myeloid lineage. IDH1 is a cytoplasmic enzyme that catalyze the oxidative decarboxylation of isocitrate to α-ketoglutarate (α-KG) in the citric acid cycle. Somatic gain-of-function mutations in IDH1 occur in ~10% of the newly diagnosed AML patients. The neo-enzymatic activity of mutant IDH1 results in accumulation of the oncometabolite 2-hydroxyglutarate (2-HG), leading to a hyper-methylation phenotype, a block in cell differentiation, and tumor growth. Inhibitors of IDH1 mutant enzyme reduce 2-HG levels and release the differentiation block allowing AML cells to achieve terminal maturation. Recently, Ivosidenib (AG120), an IDH1 inhibitor, has been FDA approved for relapsed and

newly diagnosed older AML patients. However, a subset of the mutant IDH1 AML patients treated with Ivosidenib are primary refractory or relapse while on therapy. This raises the need for development of more potent inhibitors targeting IDH1. Using a structure-based drug design approach, Lilly research laboratories developed a highly potent covalent inhibitor of mutant IDH, LY3410738.

LY3410738 modifies a single cysteine (Cys269) in the allosteric binding pocket and rapidly inactivates the enzyme, resulting in a sustained inhibition of mutant IDH1. Here we studied the pre-clinical efficacy of LY3410738 in AML cell lines engineered to express wild-type IDH1 or mutant $IDH1^{R132H}$ and in primary patient-derived AML cells harboring IDH1 mutation. LY3410738 caused rapid and more profound decrease in 2-HG levels than AG-120 in AML cells *in vitro*, translating into reversal of the differentiation block associated with IDH1 mutant activity. *In vivo*, we observed rapid and sustained 2-HG inhibition leading to a more robust and durable efficacy of LY3410738 compared to AG-120 in AML xenograft model derived from patient refractory to Ivosidenib. Since IDH1 mutant AML cells have been shown to strongly depend on the anti-apoptotic Bcl-2 for the survival, we further combined LY3410738 with FDA approved Bcl-2 inhibitor Venetoclax (ABT-199). *In vitro*, combining Venetoclax with LY3410738 demonstrated more profound reduction in cell viability and induction of apoptosis compared with single agent, in Doxycycline-inducible MOLM14/R132 cell line. Notably, the combination of LY3410738 with Venetoclax was efficacious in AML PDX xenograft models. Collectively, LY3410738 represents the first potent covalent IDH1 inhibitor that profoundly suppresses mutant IDH activity in AML cells harboring IDH1 mutation, induces differentiation and exhibits enhanced efficacy in combination with Venetoclax.

Table of Contents

List of illustrations

List of tables

Introduction:

Hematopoiesis and Leukemia formation:

Hematopoiesis is the process of blood cells formation of different lineages. This process occurs embryonically to produce the blood system and also occurs during adulthood to replace the lost blood cells or that completed their life span. All types of blood cells differentiate from the Hematopoietic Stem Cells (HSCs) which stay mainly in the bone marrow that represents the main source of the hematopoiesis in adult human. The HSCs differentiate into different progenitor cells that will differentiate into the mature blood cells. These progenitor cells are either the common myeloid progenitor cells (CMP) or the common lymphoid progenitor cells (CLP). CMPs differentiate into the megakaryocyte-erythrocyte progenitors which mature to Thrombocytes (platelets) or Erythrocytes (Red blood cells (RBCs)), the Granulocytes-macrophage progenitors (GMP) which differentiate into Neutrophils, Eosinophils or Basophils or the Monocyte-dendritic cell progenitors (MDP) which differentiate into Macrophages or Dendretic cells. CLPs differentiate into natural killer cells (NK) or lymphocytes either T lymphocytes or B lymphocytes.(1)

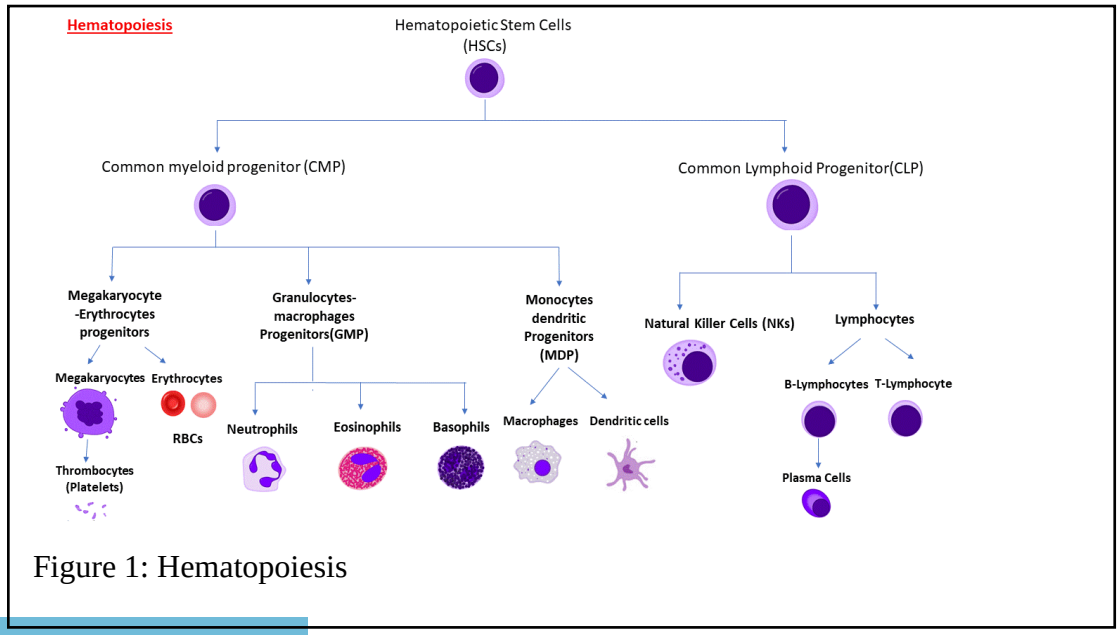

Figure 1: Hematopoiesis

The identification of multiple surface markers in the last few years enabled the isolation and identification of the HSCs, the progenitor cells and different types of blood cells using flow cytometry. Deviation of differentiation of these progenitor cells into the final mature cells, allows proliferation of immature undifferentiated cells in the bone marrow and release of the neoplastic cells into the blood.

Leukemia is a type of blood cancer characterized by proliferation of immature, undifferentiated white blood cells either Lymphocytes or Myelocytes, in the bone marrow, then releasing of these cells into the blood. The failure of blood cells differentiation could be due to many genetic abnormalities (as FLT3 or IDH mutations), or overexpression of the anti-apoptotic proteins (ex, BCL2) which inhibit apoptosis and induce cells survival. Leukemia could be acute characterized by quickly multiplication of the immature white blood cells in a short time in the bone marrow, or chronic characterized by generation of too many partially differentiated white blood cells that cannot function like mature blood cells. Chronic leukemia usually develops more slowly and is a less dramatic than acute leukemia(2).

Isocitrate dehydrogenase 1 (IDH1):

IDH1 is a cytoplasmic enzyme which catalyzes the oxidative decarboxylation of isocitrate to α-ketoglutarate (α-KG) in citric acid cycle (also known as TAC cycle or Krebs cycle), producing reduced nicotinamide adenine dinucleotide phosphate (NADPH) from NADP+. α-KG is essential for multiple dioxygenases which depend on α-KG for multiple cellular processes, including epigenetic regulation (Histone methylation and DNA methylation), hypoxia adaptation, maturation of collagens of extracellular matrix and DNA repair (3, 4).

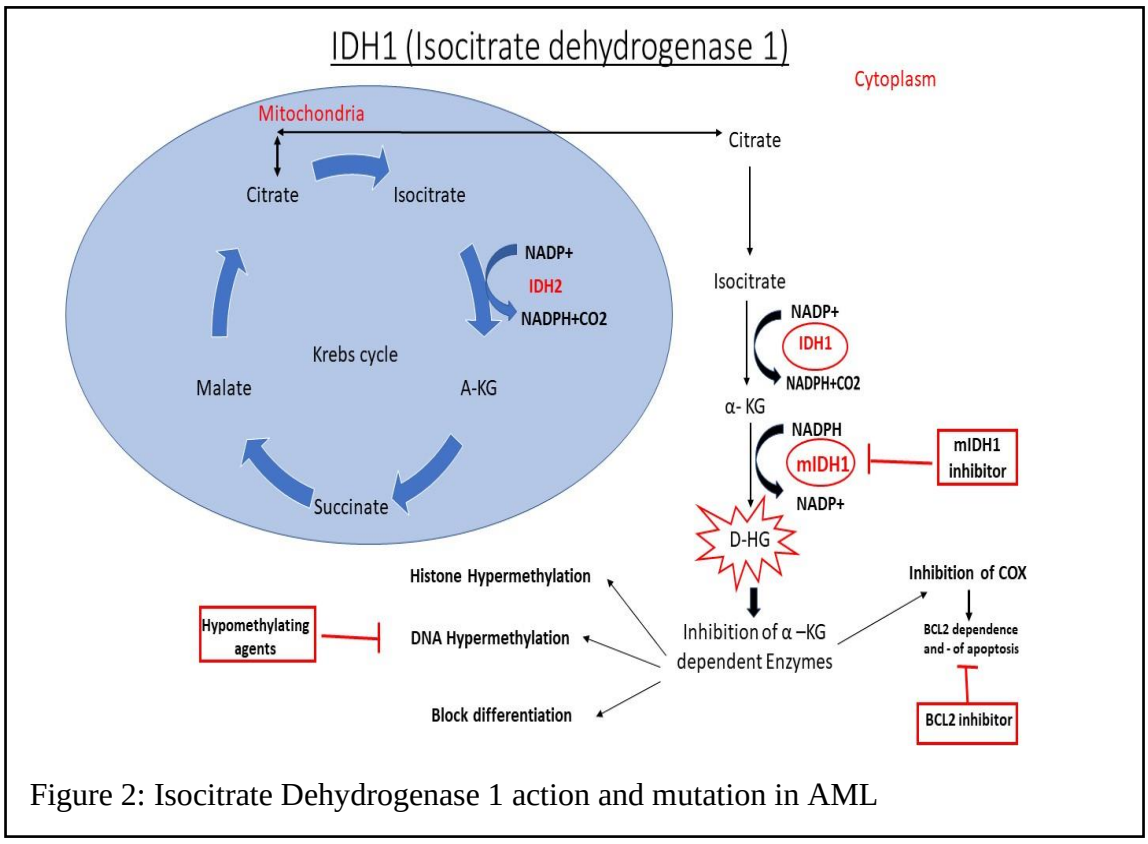

Figure 2: Isocitrate Dehydrogenase 1 action and mutation in AML

Somatic mutations in IDH1 gene on chromosome 2, have been identified in a wide spectrum of solid and hematologic malignancies including; Glioma(5), Myeloid malignancies (AML(6) , myelodysplastic syndromes (MDS), and myeloproliferative neoplasms), enchondromas and chondrosarcomas. In Myeloid malignancies IDH1 mutations are missense variants leading to histidine (R132H) or cysteine (R132C) substitution of arginine residues at R132 codon in exon 4 (7).

Somatic gain of function mutations in IDH1 enzyme let the mutant IDH1 (mIDH1) to gain neomorphic activity, converting α-KG to an oncometabolite, R 2-hydroxyglutarate ((R)-2-HG). 2HG acts as a competitive inhibitor of αKG-dependent dioxygenases, leading to disturbance in different cellular processes and epigenetic modifications. 2-HG can be used as a biomarker of the mIDH1 AML and can be used to determine the prognosis of the disease and

follow up the treatment response rate. 2-HG is detected at very low concentration in normal cells, however, is significantly elevated in tumor cells (reaching up to 10mM) and plasma of patients harboring IDH1 mutations(8)

IDH1 mutation in AML:

IDH1 mutations occur in about 10% of AML according to The Cancer Genome Atlas (TCGA) data. The presence of an IDH1 mutation alone is not sufficient for AML development. Moreover, IDH1 mutations occur together with mutations of other genes like; NPM1, FLT3-ITD, DNMT3A and KRAS/NRAS. In AML, old patients with the R132H IDH1 mutation have lower overall survival(9-11). Mutation of IDH1(R132) in AML, increases the level of the oncometabolite 2-HG. (R)-2-HG is structurally similar to α-KG and has been shown to competitively inhibit α-KG-dependent dioxygenase enzymes which are essential for DNA and Histone methylation, including members of the ten-eleven-translocation (TET) family of 5-methylcytosine hydroxylases and of groups of histone lysine demethylases. Inhibition of these epigenetic regulators by 2-HG produces a hypermethylation 'signature', which results in altering gene expression and leading to differentiation arrest of hematopoietic progenitors.(12)

Treatment of AML with mIDH1

Chemotherapy: Induction chemotherapy is the most common first line treatment of all AML patients including those with mIDH1. However, the rate of relapse is high and chemotherapy is sometimes not tolerated by patients due to the side effects. That encourages the scientists and physicians to search for targeted selective agents for treatment of AML with mIDH1 to decrease the adverse effects resulting from the chemotherapy.

hypomethylating agents (HMAs): Hypermethylation is the hallmark signature of IDH1 mutation. That makes the rational of using HMAs in the treatment of AML with mIDH1.

However, the efficacy of the HMAs used in the treatment of AML with mIDH1 is equivocal; as some studies demonstrated no association between clinical responses with HMA treatment, either with or without histone deacetylase inhibitor therapy, in the presence of mIDH1 (13). That was another reason towards developing the selective small molecules inhibitors.

Small molecules mIDH inhibitor: Nowadays there is a preference towards the precision medicine, and selective inhibition of the oncogenic mIDH1 which allows the personalized medicine through tumor gene sequencing and detection of the 2-HG oncometabolite as a biomarker to determine the efficacy of the small molecules mIDH1 inhibitor. Moreover, specific inhibition of mIDH1 have few side effects compared with the regular chemotherapy due to acting selectively against the targeted aberrant gene.

AG120 (ivosidenib): In 2018, the FDA approved ivosidenib (TIBSOVO, Agios Pharmaceuticals, Inc.) for old patients with refractory or relapsed acute myeloid leukemia (AML) with IDH1 mutation. It is a reversible non-competitive small-molecule allosteric inhibitor of mIDH-R132 protein. (14). However, a subset of AML patients with mIDH-1-R132 were primary refractory to AG120 treatment or relapsed while treatment, that makes the need to develop a new potent mIDH1 inhibitor.

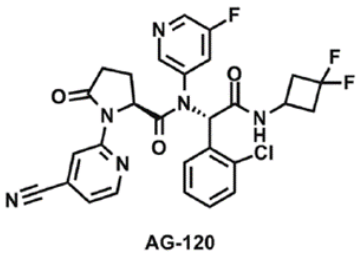

Figure 3: Structure of AG120

BCL-2 inhibitor: ABT-199 (venetoclax) is a small molecule selective inhibitor of B-cell leukemia/lymphoma 2 (BCL-2). It binds to the BH3-binding groove of BCL-2 and displaces Bim and other proteins that are normally sequestered by this anti-apoptotic protein. These BH3 proteins activate the pro-apoptotic, Bax and Bak. Bax/Bak activation then leads to mitochondrial outer membrane permeabilization and induction of apoptosis through caspases activation(15). It is proved that IDH1 mutation induces BCL-2 dependence in AML to inhibit apoptosis and keep cell survival through inhibition of Cytochrome c Oxidase (COX), the hallmark of mitochondrial apoptosis, which induce the BCL-2 (anti-apoptotic) dependence. BCL-2 maintains the cell viability by antagonizing the pro-apoptotic BAX/BAK activation. (16).

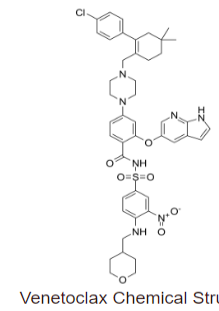

Figure 4: Structure of ABT-199

LY3410738

A novel, oral potent covalent inhibitor of mutant IDH1, developed with Eli Lilly and Company, using a structure-based drug design approach. LY3410738 modifies a single cysteine (Cys269) in the allosteric binding pocket and rapidly inactivates the enzyme with a KI/Kinact = 84,257 M-1sec-1. The compound selectively inhibits the 2-HG in IDH1 mutant tumor cells without depleting the levels of a-ketoglutarate.

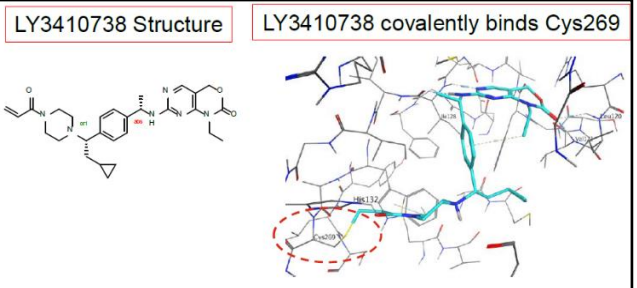

Inhibition kinetics of IDH1/R132H by LY3410738

LSN	k_{inact} (min^{-1})	K_I (nM)	k_{inact}/K_I ($M^{-1}Sec^{-1}$)	$t_{1/2}^{\infty}$ (min^{-1})	Time for >95% inactivation
3410738	0.1583	31.2	84257	4.38	22 min

Figure 5: LY34110738 Structure.
Eli Lilly and Company AACR 2019

Hypothesis and Research aims:

Hypothesis

LY3410738 drug rapidly inactivates mIDH1-R132H enzyme in AML patients, it will act faster and more durable than AG120 resulting in better response rates. Combining this inhibitor with ABT-199 (BCL-2 inhibitor) will improve its antileukemic effect in AML patients.

Aims:

Aim1: Examine molecular mechanisms of IDH1 inhibitor LY3410738 *in vitro* compared with AG120.

Aim 1-a. Examine molecular mechanisms of IDH1 inhibitor *in-vitro* in the engineered THP-1/R132 cell line and MOLM 14 /R132 cell line compared with the action of AG120 drug.

Aim 1-b. Examine molecular mechanisms of IDH1 inhibitor LY3410738 *in-vitro* in primary AML patient samples cultured for 7 days in vitro.

Aim 2: Establish the anti-leukemia efficacy of the novel IDH inhibitor in AML PDX *in vivo* models compared with AG120.

Aim 2-a. The anti-leukemia activity will be assessed by tumor cells measurements in blood and mice survival. Induction of differentiation will be determined by flow cytometry for differentiation markers (CD15, CD14 and CD11b) in peripheral blood (PB). The levels of 2-HG will be determined.

Aim 2-b. Changes in gene expression and methylation will be determined through RNAseq analyses and methylation assays.

Aim 3: To test the combination of novel IDH1 inhibitor with targeted agent BCL-2 selective antagonist ABT199.

Aim 3-a. *In vivo*: PDX model will be established with IDH1-mutant AML. The anti-leukemia activity will be assessed by tumor burden measurements (serial CD45+/CD33+ flow cytometry, every 2 weeks) and mice survival. Induction of differentiation will be determined by flow cytometry using differentiation markers (CD11b, CD14 and CD15) in PB. Levels of 2-HG will be determined. Effects on DNA methylation will be assessed using Illumina EPIC Micro-array.

Aim 3-b. *In vitro*: combination effect will be tested in the engineered THP-1/R132 cell line and MOLM14/R132 cell line by measuring the Viability with CellTiter-Glo® Luminescent Cell Viability Assay and with Flow cytometry using Annexin V.

Methods and Materials:

In-Vitro:

Cell Lines and Cell culture:

Molecular mechanisms of IDH1 inhibitor LY3410738 were examined *in vitro* in the engineered doxycycline-inducible THP-1/R132 cell line (kindly provided by S. Chan, U. Toronto)(16). Cells were induced with 2µg/ml Doxycycline for 4 days, then were treated with LY3410734 or AG120 for 4 days.

Mechanisms of IDH1 inhibitor LY3410738 were examined *in vitro* in the engineered doxycycline-inducible MOLM14-R132 cell line (Kindly provided by J. Sarry, Toulouse, France). Cells were induced with 2µg/ml Doxycycline for 4 days, then were treated with LY3410734 or AG120 for 4 days.

Cells were cultured using RPMI media with 10% FBS and 1% Penicillin/ Streptomycin. And incubated at 37c degree.

Measuring the level of 2-HG and alpha KG by liquid chromatography-mass spectrometry (LC-MS):

The effects of IDH1 inhibition by LY3410738 on the concentrations of total 2HG were determined by liquid chromatography-mass spectrometry (LC-MS) analysis of the media collected from the cells. 100,100 cells were incubated in 24 well plates at 37c after induction with doxycycline after treated with the drugs for four days, then 65µl of the media were collected in 1.7 Eppendorf tubes and centrifuged at 300g for 5 min, the 60µL of the supernatant were collected and put at 96 well plates and feezed at -80c then shipped to Lilly research laboratories to be analyzed with LC-MS.

Cell Count, Viability and Cells Differentiation

Cell count and Viability are measured using Trypan blue which is an azo dye, used as vital stain to selectively color dead tissues or cells blue. Live cells or tissues with intact cell membranes are not colored.

Effects on differentiation using phorbol 12-myristate 13-acetate (PMA) (50 nM/200 µL, in 96 well plate after another 5 days), (17) were studied. It is known that PMA differentiate THP1 cell line into macrophage (Monocytes)which attach to the wells after differentiation. We have tested the effect of IDH1 mutation on blocking the differentiation induction and the effect of the novel IDH1 inhibitor on the release of the block in definition. Induced cells cultured for 5-8 days with PMA, then the media was discarded and the wells were washes with PBS twice and the attached cells were counted using Siligo Microscope [17].

In studying the combination efficacy, we tested the viability with trypan blue (% of viable cells). We also used CellTiter-Glo® Luminescent Cell Viability Assay (CTG Assay) which is a method of determining the number of viable cells in culture based on quantitation of the ATP present, an indicator of metabolically active cells. We also used the flowcytometry to test the viability using Annexin V/DAPI assay, with counting beads. Annexin V is a cellular protein used in Flowcytometry to detect apoptotic cells by its ability to bind to phosphatidylserine, a marker of apoptosis when it is on the outer leaflet of the plasma membrane. Annexin V bonded to APC fluorochrome (Annexin V APC, Biolegend #640941). DAPI (Invitrogen by Thermo Fisher Scientific, Ref# D3571). Cells collection stopped when counting beads reach 250 beads per sample. Kalusa software was used for analysis. The percentage of gated Annexin V -ve/ DAPI -ve cells were considered the Viability %. While Annexin V +ve (APC +ve) cells percentage were considered the apoptosis %.

Patient samples:

Patient sample was provided from MD Anderson Cancer Center's leukemia clinic after taking patient's consent. Molecular mechanisms of IDH1 inhibitor LY3410738 were examined in primary AML patient samples with mIDH1/R132, cultured for 7 days. Effects on 2-HG level and differentiation were studied in media. Viability was examined with Trypan Blue, APC Annexin V and DAPI. Differentiation was examined using differentiation markers (hCD14, hCD15, hCD11b). Patient samples cultured in Stem spam Media (Stem cell Technologies Ref# 09650) with 20 ng/ml FLT3-ligand, 50 ng/ml SCF, 20 ng/ml TPO, 20 ng/ml IL3, 20 ng/ml IL6 and 1fold of penicillin/Streptomycin (Protocol provided with Elli-Lilly and Company).

Western Blot:

Effects on the protein levels of Wild type (wt). and mutant IDH1 and histone methylation were examined by immunoblotting (WB). Cells collected in 15 ml falcon tubes, centrifuged at 1500 rpm for 5 min, then washed with 2 ml DPBS and centrifuged, 100 µL of RIPA buffer (Pierce TM RIPA BUFFER: LOT: TG269912, Thermo scientific USA, REF# 89900) with Protease/phosphatase Inhibitor Cocktail (ref: 5872S, Cell Signaling) and left for 30 min, then collect the protein supernatant. Running: used 4-20% gel (Mini-PROTEAN TAX Precast Gels, Cat# 456-1096, 15µl/well, Bio-Rad Laboratories), Running buffer Tris/Glycine/SDS Buffer 10x, BioRAD, Cat# 1610772), running for 1 hour starting with 80 V then increase to 120 V. The transfer: Immobilon-P Transfer membrane Cat # IPVH00010, transfer machine: BIO-RAD PowerPac Basic, Transfer at 220 MA for 80 min, using transfer buffer: Tris-Glycine Transfer Buffer 40x, Novex, lot# 2080927, ref# LC3675 (760 ml H2O, 200 ml methanol, 40 ml Transfere buffer). Then blocking for one hour, then adding the primary Antibody in blocking buffer 1:1000, left overnight. Then wash with TBST three times, and add the

secondary antibody in blocking buffer 1:15000, and left for one hour then washed with TBST four times and then the image was taken. Bands were measured using image studio.

Primary antibodies used: Histone H3 Mouse mAb (cell signaling, cat# 14269S), Tri-Methy-Histone H3 (K27) Rabbit mAb (cell signaling, cat# 9733T), Tri-Methyl-Histone H3 (Lys9) Rabbit mAb (Cell Signaling, cat# 13969T), TRI-Methyl-Histone H3 (K4) Rabbit Ab (cell signaling, cat# 9727S), IDH1 mAb Rabbit (Cell Signaling, cat# 3997S), Anti-IDH1 (R132H) Ab, Mouse monoclonal (Sigma).

In vivo:

Compounds:

IDH1 inhibitor, LY3410738 lot# ATP-E16094-010-7, was produced and provided by Eli Lilly and Company, and Lilly Research Labs. Each test article was prepared at an appropriate concentration with vehicle to give animals the doses tested in this study at a dosing volume of 10 µL/gram body weight. The formulation used for LY3410738 was Acacia vehicle (water, 10% Acacia, 0.05% Antifoam [Dow Corning 1510-US] with 1.1 molar eqivalents HCl (per molar LY3410734 conc.). All dosing solutions of the test articles were prepared in their specific formulation once every 7 days and stored at 4°C between doses.

IDH1 inhibitor, AG120 lot# AAL-Z16035-117-1, were provided by Eli Lilly Company, Purchased from Agios Company.

ABT-199: 50 mg/kg QD. Cat. N0. V-3579, Lot# VNT-113, was provided from Elli Lilly company, purchased from LC Laboratories Wc. Is formulated in a mixture of 60% Phosal 50 PG (http://www.americanlecithin.com/TDS/TDS_50PG.pdf), 30% PEG 400, and 10% EtOH. The most effective method of formulation is to add the appropriate volume of EtOH to the

appropriate mass of powder and mix by vortexing very well. Make certain that there are no large clumps of compound on the bottom of the bottle. Re-suspend any large clumps carefully with a pipette. A uniform cloudy suspension should be achieved. The appropriate volumes of PEG 400 and Phosal are then added and the solution is mixed by vortexing. Allowing the suspension to sit for ~30 min after adding all the excipients may help to achieve uniformity. Daily oral dosing for 15 consecutive days has been shown to be well tolerated in multiple strains of mice. The vast majority of our studies have been done in female NSG mice. The drug will be very viscous and not in solution in this vehicle, so care (and patience) is required for oral gavage. Shake well before dosing. Our typical dosing volume is 0.1 ml with the drug given at 50 mg/kg/day, once a day for up to 15 consecutive days. Compound is typically made fresh every 5-7 days and should be stored in a brown or amber bottle to protect from light at room temperature.

Human IDH1(R132H) AML PDX Mouse Model and Treatments

Human patient derived AML cells were implanted into mice to establish the model. The leukemia was passaged and propagated in NSG mice by Konopleva's Research Lab to establish the stable model using the procedures detailed below. A mouse implanted with human IDH1(R132H) AML cells from this model. The spleen was removed using standard technique and protocol by our lab. The spleen was placed in ice cold sterile PBS in a 15 mL collection tube (spleen was significantly enlarged due to a high leukemic burden in this mouse). The spleen was removed from the collection tube and placed in a 50 mL conical tube. The spleen was processed by gentle rubbing of the spleen tissue against the surface of the cell strainer (using a filter) with the end of a 5 mL syringe plunger in a circular motion. The filter was rinsed with 10 mL room temperature sterile DPBS 3 times during the process. After no intact

spleen tissue was visible, a final rinse of the filter was performed and the cell prep was mixed up and down multiple times, using a 10 mL sterile serological pipette. The cell pellet was collected by centrifugation (RPM 1500 for 5 min) then using 5 µL of Lysis buffer and shacked for 5 min then washed two times with 40 mL sterile DPBS. The cells were counted and resuspended in DPBS at the desired implant concentration or freezed in 10%DMSO and 90% FBS. One hundred µL per mouse was injected IV (intravenous, tail vein) into naïve NSG mice (irradiated one day prior to implant [2.5 Gy]). Whole blood samples were collected after 3-4 weeks by eye bleed (<100 µL) and analyzed by Gallios Flow cytometry (FACS) for the presence of human CD45+ cells and %AML determined (%AML was determined as the % human CD45+ white cells of total white cells). Once the leukemia in the study mice was confirmed positive by FACS analysis (>0.5-1% AML of total white cells), the mice were randomized by % leukemia and placed into treatment groups. Leukemic mice were treated 10 mg/kg LY3410738 PO QD. Blood samples were collected biweekly by eye bleed (<100 µL), and analysis performed by FACS, to monitor differentiation state and leukemic burden in the study mice. LY3410738 treated mice were assessed in comparison to vehicle treated and naïve (non-tumor bearing) control mice. Body weight was recorded once a week.

Whole Blood FACS Analysis and Plasma Collection

Whole blood samples (<100 µL) were collected biweekly by eye bleeding, into K-EDTA blood collection tubes over the course of the study. Fifty to seventy µL of whole blood was aliquoted into 1.5 mL microfuge tubes for each subject and spun at 300 x g for 10-12 minutes (4°C). Ten µL of plasma was collected and transferred to new 1.5 mL microfuge tubes and frozen at -80°C for 2HG LCMS analysis

Sixty µL stain/wash buffer (5% heat inactivated (HI)-FBS(v/v) (Invitrogen 10082) in DPBS (HyClone SH30028)) was added per tube, mixed up and down 3 to 4 times by pipette, and 100 µL of the blood suspension was transferred to 5 mL polypropylene tubes. The stains were added according to the manufacturer's instructions (anti-human CD33-APC (BD Biosciences cat#551378), anti-human CD14-PE-Cy7 (BD Biosciences cat#557742), anti-human CD15-V500 (BD Biosciences, cat#561585), anti-human CD45-APC-Cy7 (BD Biosciences cat#557833). The samples were incubated for 30 minutes at room temperature, protected from light. After the incubation, 1.5 mL 1X BD Lyse/Fix (37°C, (BD#558049)) was added to each sample and incubated for 12 minutes at room temperature. The tubes were then centrifuged at 1500 RPMI for 5 minutes. BD Lyse/Fix solution was aspirated and the cell pellet washed with stain/wash buffer 2 times. Fixed cells were then resuspended in 300 to 400 µL stain/wash buffer then transferred to filtered flow tubes. Samples were analyzed on a Gallios Flow cytometer (Beckman, Texas) using standard flow cytometry principles and techniques. It is best practice to analyze the samples on the same day as they are stained and fixed. Population gating and data analysis of percent population were performed in the Flow Jo software. Percent population values from the data analysis were plotted in GraphPad Prism.

LCMS Analysis of Plasma Samples, protocol done with Eli-Lilly and Company.

The effects of IDH1 inhibition by LY3410738 on the concentrations of total 2HG were determined by liquid chromatography-mass spectrometry (LC-MS) analysis of mouse plasma samples from a patient-derived xenograft model of AML. Whole blood samples were placed into EDTA collection tubes and centrifuged at 300g for 10-12 min to isolate the plasma. Then 10 µL of plasma is collected from each sample at Eppendorf and freezed at -80 till shipping in dry ice to Lilly research laboratories. Ten µL of each plasma sample were placed into a deep-

well 96 well plate and combined with 100 µL of internal standard solution containing 10 µM 3-hydroxy-1,5-pentanedioic-2,2,3,4,4-d5 acid (d5 3HG, Sigma). One hundred twenty µL of methanol and 90 µL of chloroform are added to each sample. The plate was sealed, vortexed for 5 minutes, and centrifuged for 10 minutes at 4000 rpm on in Eppendorf 5810R centrifuge. One hundred fifty µL of the upper layer were transferred to a new 96 well plate and dried under heated nitrogen at 50°C. The samples were derivatized by adding 100 µL of 1 M O-benzylhydroxylamine in pyridine buffer (8.6% pyridine, pH 5) and 100 µL of 1 M N-(3-dimethylaminopropyl)-N-ethylcarbodiimide hydrochloride (EDC) in pyridine buffer to each sample. The derivatization reaction proceeded at room temperature for 1 hour. Using a Beckman Biomek FX liquid handler 300 µL of ethyl acetate was added to each sample. Plates were sealed and vortexed for 5 minutes, then they were centrifuged for 5 minutes at 4000 rpm. Two hundred twenty µL of the upper layer were transferred to a new 96 well plate. Samples were dried under heated nitrogen at 50°C and reconstituted with 100 µL of methanol/water (1:1). Ten µL of derivatized sample was injected onto an LC-MS system consisting of a Shimadzu Prominence 20A HPLC system and a Thermo Quantum Ultra™ triple quadrupole mass spectrometer. Analytes were separated on a Water XBridge™ C18 column (2.1 x 50 mm, 3.5 µm) with a flow rate of 0.6 mL/minute. Mobile phase A was 0.1% formic acid in water and mobile phase B was methanol. The gradient profile was: 0 minutes, 5% B; 2 minutes, 100% B; 4 minutes, 100% B; 4.1 minutes, 5% B; 5.50 minutes, stop. The mass spectrometer utilized a HESI-II probe operated in positive ion selected reaction monitoring mode. The precursor and fragment ions for the derivatized analytes were: 2HG (359→91), d5-3HG (364→241). Calibration curves were constructed by plotting analyte concentrations versus analyte/internal standard peak area ratios and performing a quadratic fit of the data using

a 1/concentration weighting with Xcalibur™ software. Analyte concentrations for the unknowns were back-calculated from the calibration curves.

DNA and RNA preparation

Human leukemia cells were extracted from mice's spleens, and sorted from mice cells using STEMCELL, EasySteptm Mouse/Human Chimera Isolation Kit (Catalog # 19849A, Lot# 18M98260) and magnetic beads, the DNA was extracted using QIAGEN, QIAamp DNA Mini Kit (50), REF: 51304. DNA methylation essay was done at the Microarray Core facility MD Anderson Cancer Center to check for DNA methylation by EPIC Microarray. Analysis was done using cluster analysis software, P-Value: 0.05.

RNA was extracted using QIAGEN, ALL prep RNA/Protein Kit (50) Cat. 80404, and sent for RNA Sequencing at Novogene Company. RNA seq was done using Homo Sapiens Human genome 38 as a reference. Cluster profile software for enrichment analysis. Cut off is p=0.05.

Definitions:

GO: gene ontology (A major bioinformatics initiative to unify the representation of gene and gene product attributes across all species) It includes three main branches: cellular compares (CC), molecular function (MF) and biological process (Bp)

DO: The Human Disease Ontology (is a community driven standards-based ontology)

UP: upregulated differential genes

Down: downregulated differential genes

Barplot, Horizontal axis showed -log10(padj) value of certain GO term. Vertical axis showed the number of genes of this term.

Results:

In-Vitro

Aim1-a: Examine molecular mechanisms of IDH1 inhibitor LY3410738 in vitro compared with AG120.

Doxycycline induction increases the level of 2-HG in the mutant IDH1/R132 THP1 and MOLM14 cell lines compared with the Wild Type cells in-vitro.

To test the effect of the IDH1 inhibitor on the level of 2-HG we tested first the level of 2-HG after induction of the IDH1 enzyme with 2µg/ml Doxycycline for 4 days in THP1/R132 and MOLM14/R132 engineered cell lines. Doxycycline induction demonstrated time dependent increase in the level of 2-HG (Figure: 6A) associated with increase in the number of the mutant THP1/R132 cells compared with THP1 WT (Figure: 6B). After 4 days of induction with doxycycline, the level of 2-HG is significantly higher in the media collected from the IDH1 mutant cells compared with IDH1 WT (Figure: 6C).

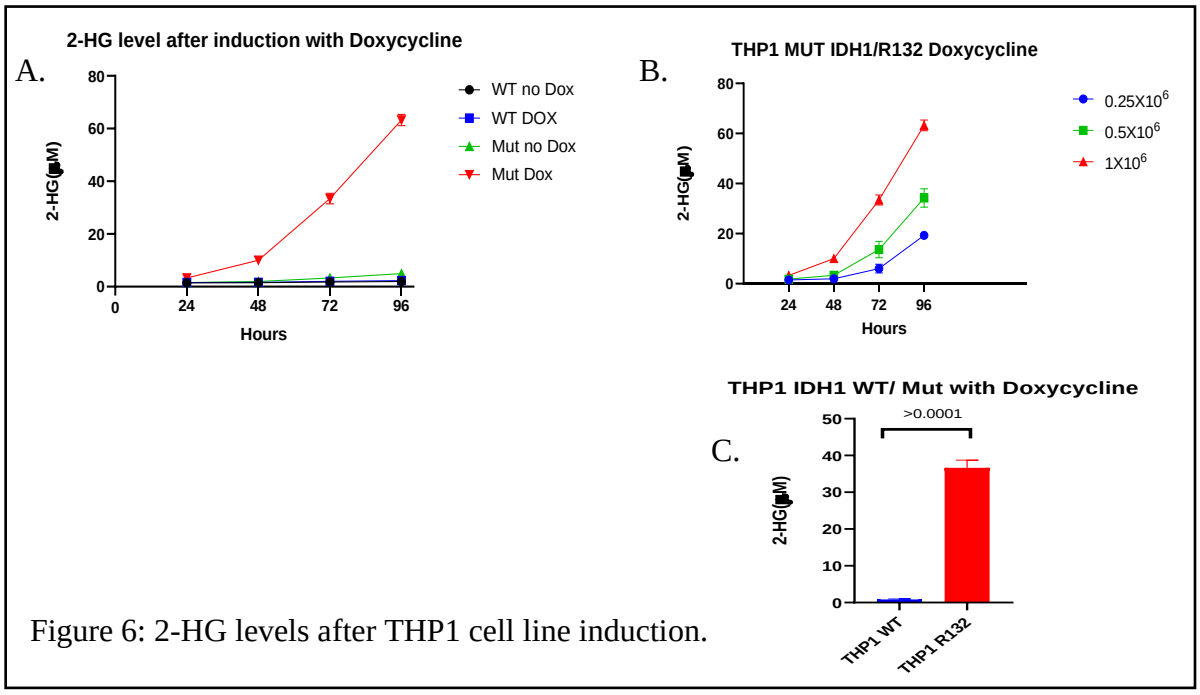

Figure 6: 2-HG levels after THP1 cell line induction.

Also, MOLM14/R132 induced with 2µg/ml Doxycycline demonstrated time dependent increase in the level of 2-HG (Figure 7A). After 4 days of induction with doxycycline, the level of 2-HG is significantly higher in the media collected from the IDH1 mutant cells compared with IDH1 WT (Figure 7B).

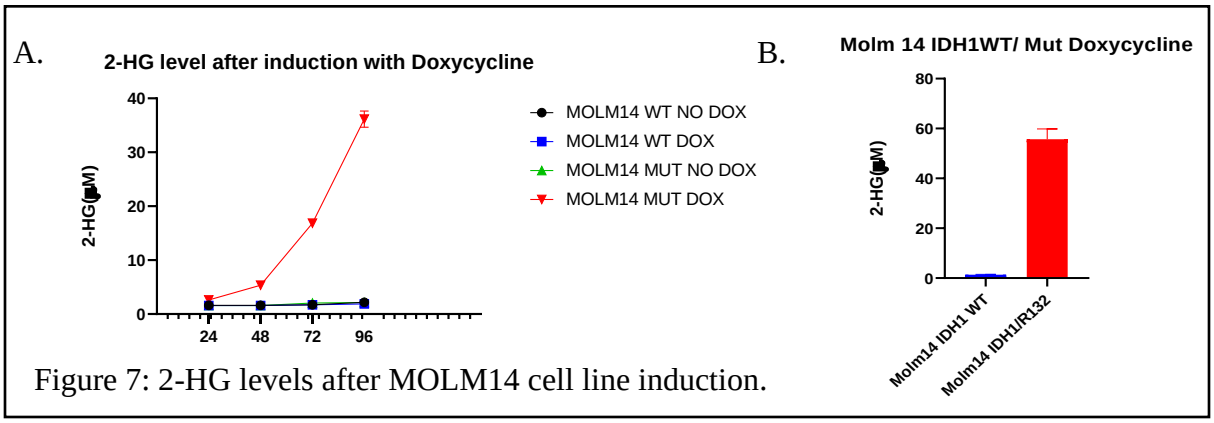

Figure 7: 2-HG levels after MOLM14 cell line induction.

LY3410738 Drug induced decrease in 2-HG earlier and with smaller dose, compared with AG120

Doxycycline induced THP1/R132 cell line treated with 0.1 or 1 µM LY3410738 for 4 days induced Significant reduction of the level of 2-HG. LY3410738 induced a rapid and significant reduction of the 2-HG level with lower dose (0.1µM) compared with AG120 (Figure 8).

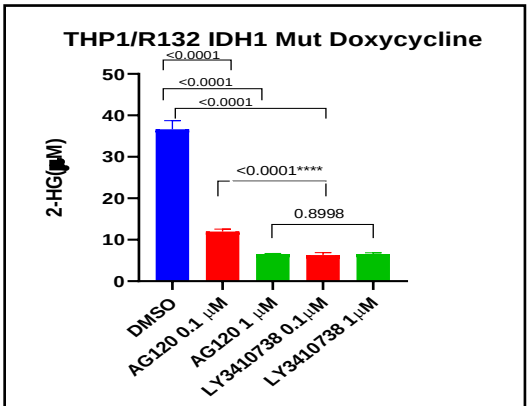

Figure 8: Early reduction of 2-HG level after LY3410738 treatment in THP1/R132 cell line.

LY3410738 also induced a rapid and significant reduction of the 2-HG level with lower dose (0.1µM) compared with AG120 in induced MOLM14/R132 treated with the agents for 4 days (Figure 9).

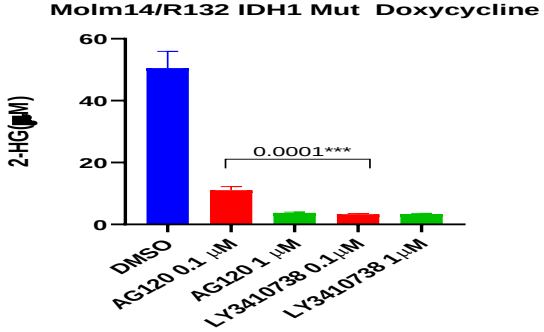

Figure 9: Early Reduction of 2-HG level after treatment with LY3410738 in MOLM14/R132 cell line.

LY3410738 induced Histone hypomethylation in both THP1/R132 and MOLM14/132 cell lines.

IDH1 WT and IDH1/R132 proteins were detected after induction with 2µg/ml Doxycycline for 4 days compared with the non-induced cells. Expression of inducible mutant IDH1 is associated with histone hypermethylation. LY3410738 caused histone hypomethylation of H3 K9me3, H3 K4me3, after treatment with 1 µM of the LY3410738 drug or AG120 for 4 days in THP1/R132 cell line (Figure: 10 A) and MOLM14/R132 cell line (Figure: 10 B).

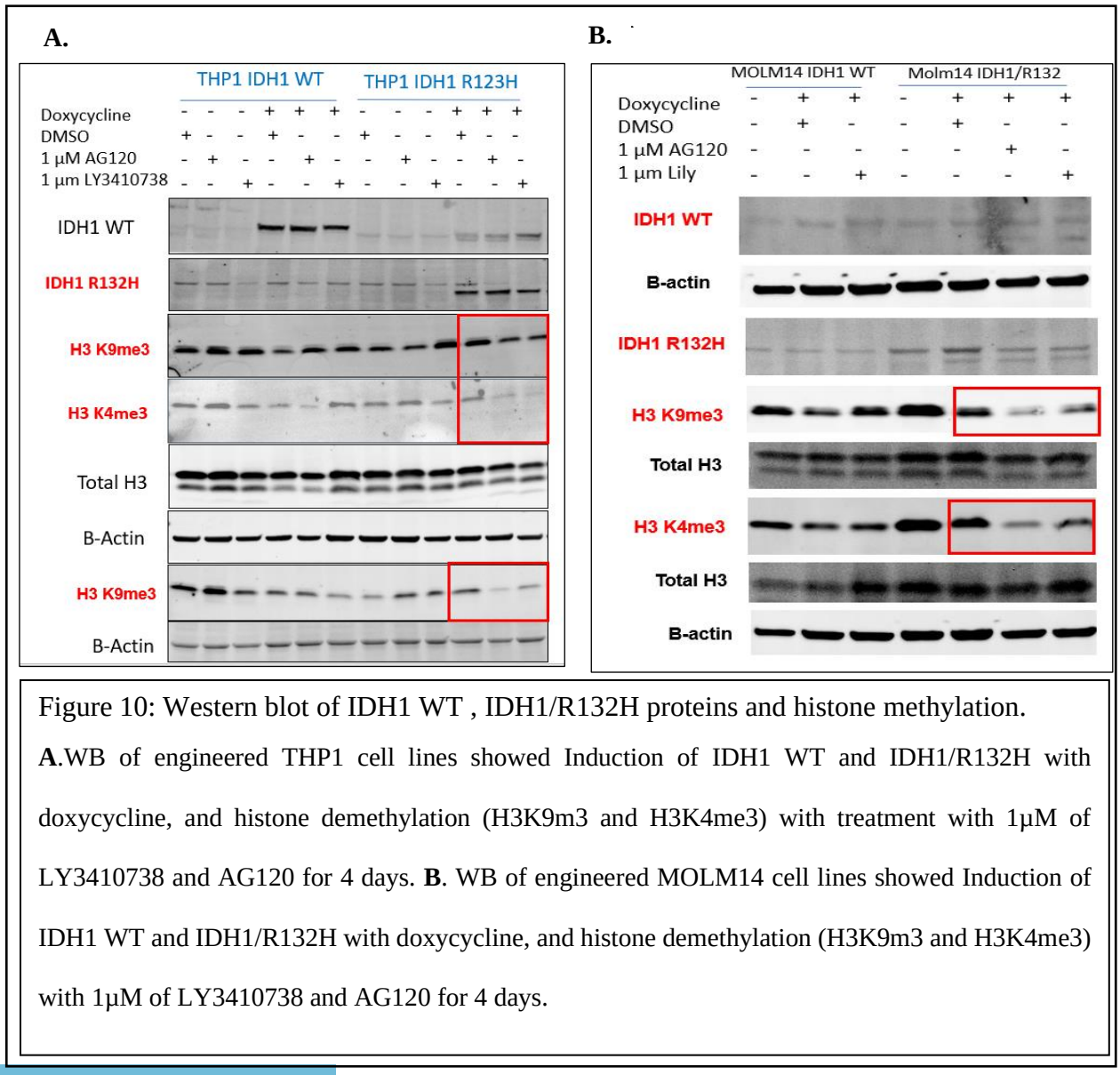

Figure 10: Western blot of IDH1 WT , IDH1/R132H proteins and histone methylation.

A.WB of engineered THP1 cell lines showed Induction of IDH1 WT and IDH1/R132H with doxycycline, and histone demethylation (H3K9m3 and H3K4me3) with treatment with 1µM of LY3410738 and AG120 for 4 days. **B**. WB of engineered MOLM14 cell lines showed Induction of IDH1 WT and IDH1/R132H with doxycycline, and histone demethylation (H3K9m3 and H3K4me3) with 1µM of LY3410738 and AG120 for 4 days.

LY3410738 induced further differentiation of mIDH1 THP1 cells stimulated by PMA Differentiation Essay.

To study the effect of the novel IDH1 inhibitor LY3410738 on induction of differentiation, we have induced the THP1 WT and THP1/R132 cell lines with 2µg/ml Doxycycline for 4 days, then treating the cells with 1 µM of the IDH1 inhibitor either LY3410738 or AG120 for 4 days. Then, 50 nM/200 µL PMA were added, in 96 well plate for another 5 days. Pictures were taken for wells, then pictures were taken after suction of the media and wash with BPS twice. Attached cells were counted using Celigo Microscope by using the confluence of the wells. PMA differentiation Essay demonstrated significant decrease in differentiation in mutant THP1 induced with IDH1 mutation and significant induction of differentiation with the novel LY3410738 IDH1 inhibitor compared with AG120 (P=0.0130). (Figure 11)

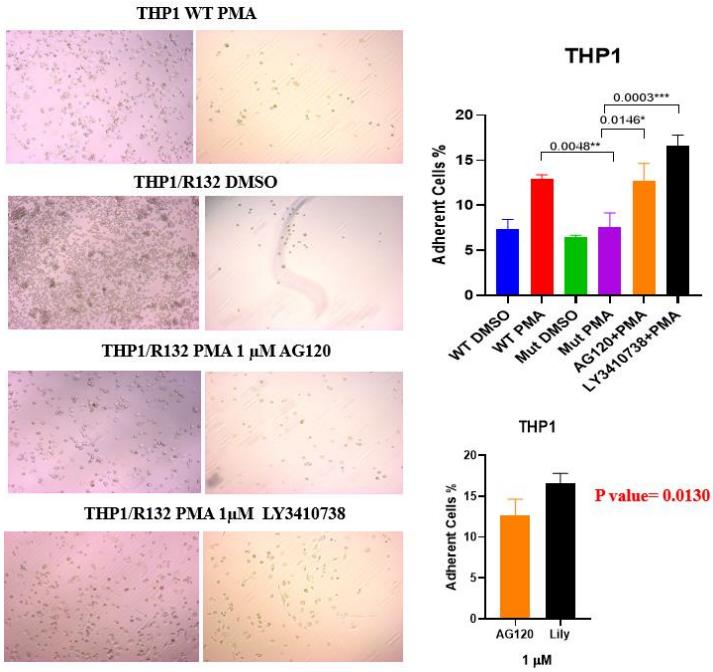

Figure 11: PMA differentiation Assay in THP1 cell line

Induction of differentiation was studied using flowcytometry, however, differentiation was not clear using flowcytometry. Induction of the cell line with Doxycycline interfered with the flowcytometry use.

LY3410738 induced some further differentiation of mIDH1 MOLM14/R132 cell line detected with flowcytometry

Doxycycline induced MOLM14/R132 cell line demonstrated induction of some differentiation of leukemic cells into CD15+ (Figure 12A) and CD14+ cells (Figure 12B), with treatment with 1 µM LY3410738 for 4 days. But no significant difference was detected compared with AG120.

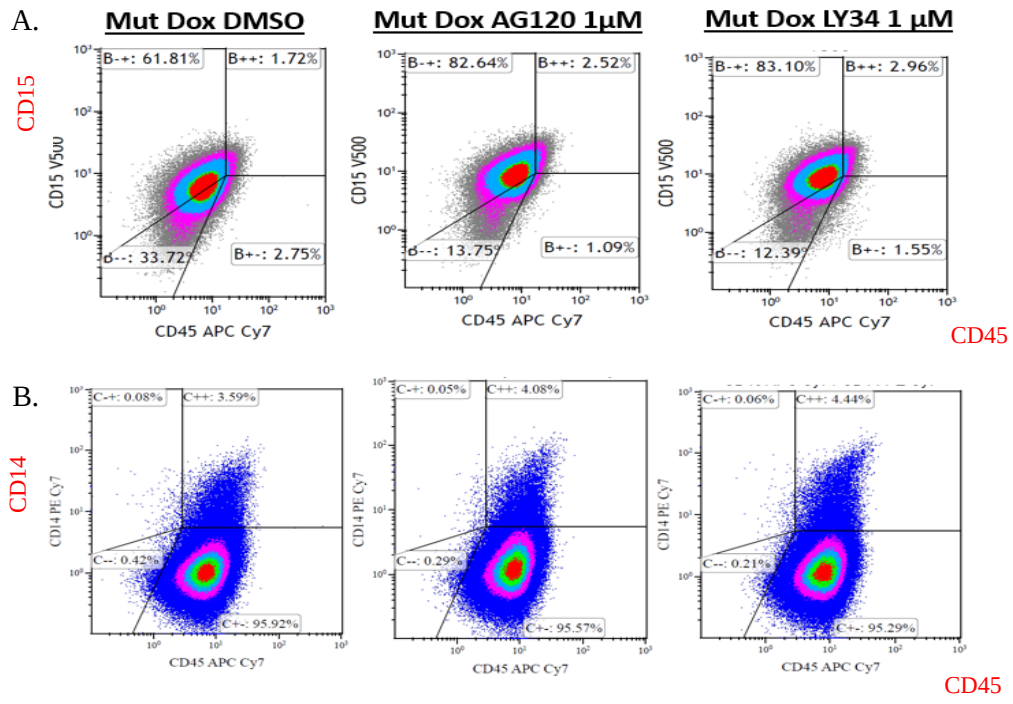

Figure 12: Induction of differentiation in MOLM14/R132 cell line detected with flowcytometry.

A.CD15 differentiation marker detected in MOLM14/R132 cell line treated with DMSO, 1µM AG120 or 1µM LY3410738 for 4 days. B. CD14 differentiation marker detected in MOLM14/R132 cell line treated with DMSO, 1µM AG120 or 1µM LY3410738 for 4 days

Aim 1-b. Examine molecular mechanisms of IDH1 inhibitor LY3410738 in-vitro in primary AML patient samples cultured for 7 days in vitro.

LY3410738 reduced 2-HG levels and induced differentiation in-vitro in AML patient sample #1 refractory to AG120.

To test the efficacy of the novel IDH1 inhibitor LY3410738 in-vitro, we used primary AML patient sample with mIDH1/R132H (clinically refractory to AG120) treated with LY3410738 for 7 days, and we tested the effect on 2-HG levels in media of cultured cells treated with different doses (0, 0.012, 0.037, o.111, 0.333, and 1µM) of LY3410738 compared to AG120. LY3410738 induced rapidly reduction of 2-HG levels with lower concentrations (Figure 13A) compared with AG120 (Figure 13B)

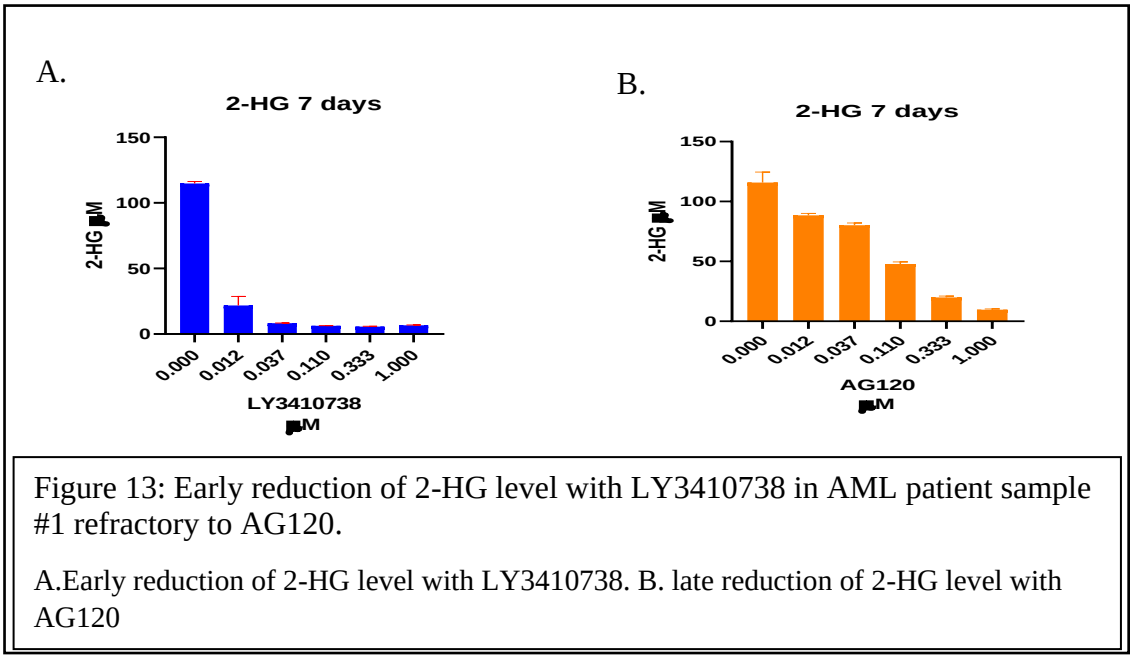

Figure 13: Early reduction of 2-HG level with LY3410738 in AML patient sample #1 refractory to AG120.

A.Early reduction of 2-HG level with LY3410738. B. late reduction of 2-HG level with AG120

Induction of differentiation was noticed with increasing doses of LY3410738 through increase in hCD15+ (Figure 14A) and hCD14+ (Figure 13B) cells percentages, detected by flowcytometry in primary AML patient sample#1 with mutant IDH1/R132H, refractory to AG120 treatment.

Patient sample #1

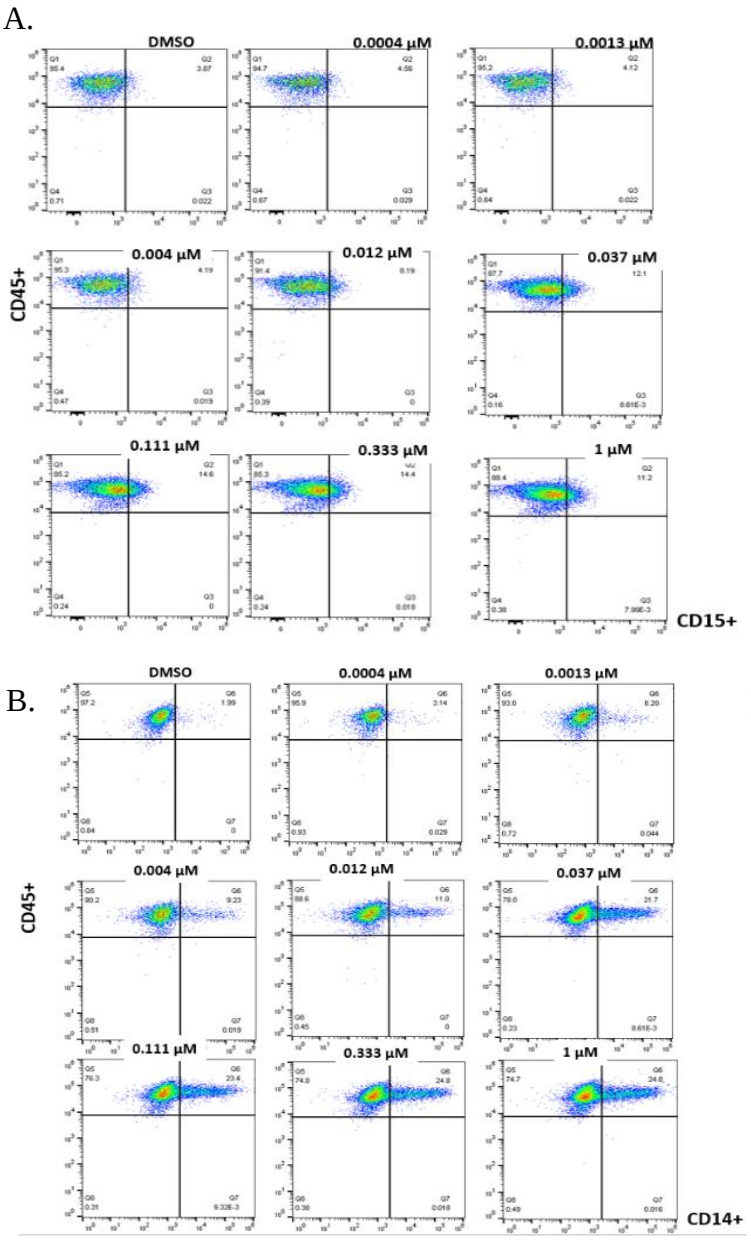

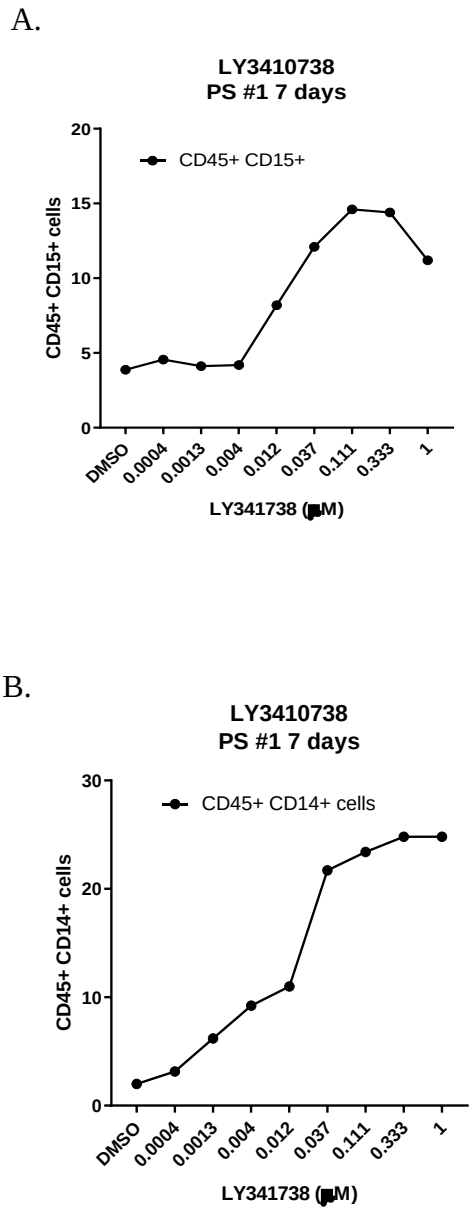

Figure 14: Induction of differentiation with LY3410738 in primary AML patient sample #1 refractory to AG120.

A.Increase in CD15 marker with increasing doses of LY3410738. B. Increase in CD14 marker with increasing doses of LY3410738

We tested the efficacy of the novel IDH1 inhibitor LY3410738 in-vitro in other primary AML patient samples (Figures 15 &16) treated with LY3410738 for 7 days but no significant deference was found in the differentiation markers compared with DMSO.

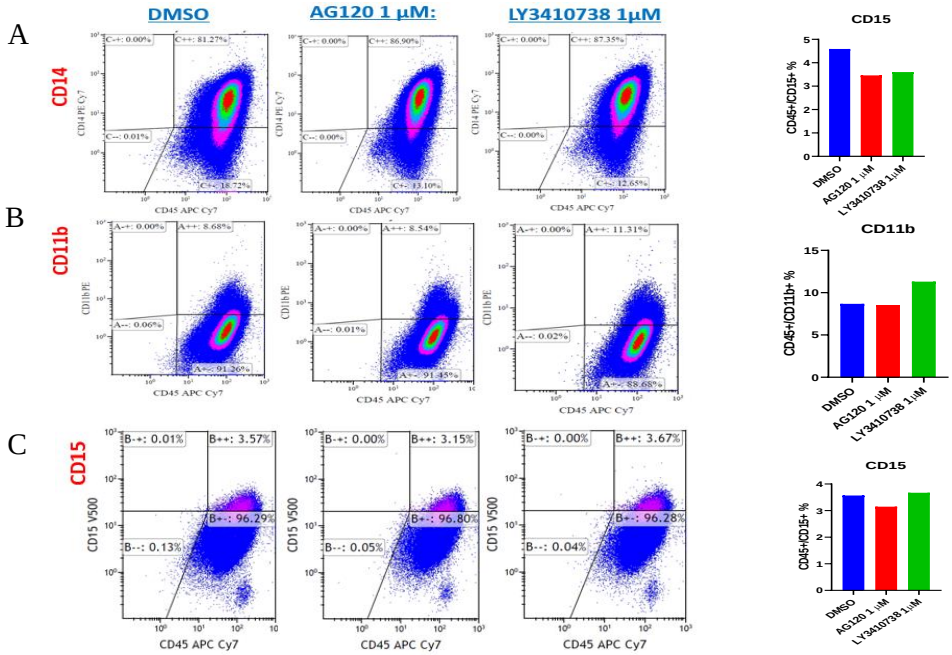

Figure 15: Differentiation markers in AML patient sample #2.

A.No significant difference in CD14 level between DMSO, 1µM AG120 or LY3410738. B. Small increase in CD11b induced with LY3410738 compared with DMSO and AG120. C. No significant difference in CD15 level.

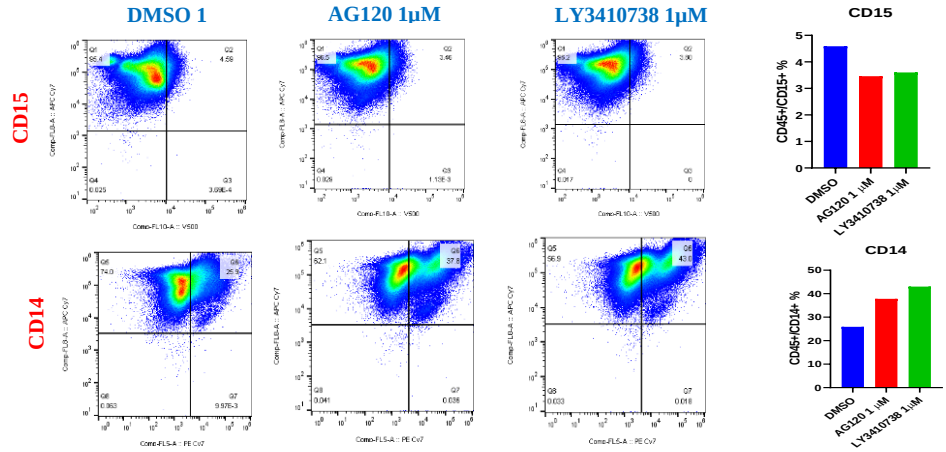

Figure 16: Differentiation markers in AML patient sample #3. A.No significant difference in CD15 level between DMSO, 1µM AG120 or LY3410738. B. Small increase in CD14 induced with LY3410738 compared with DMSO and AG120.

In-Vivo

Aim 2a: To Establish the anti-leukemia efficacy of the novel IDH inhibitor in AML PDX in vivo models compared with AG120.

LY3410738 induced differentiation and reduction of tumor burden in mice PDX model refractory to AG120.

Primary AML cells (FLT3-ITD, DNMT3A, **IDH1/R132H**, KIT, NPM1) collected from patient refractory to Ivosidenib (AG120) treatment, were injected iv into irradiated NSG mice, and engraftment was monitored by CD45 flow cytometry. Upon documenting the engraftment (>1% circulating Human AML cells) mice were grouped into 3 groups (8 mice/group for efficacy studies. In addition, we set an additional cohort of 6 mice (3 control, 3 treated) for PD studies). Mice were orally gavaged with the IDH1 inhibitors (either AG120 or LY3410738) 10mg/kg once daily. The anti-leukemia activity was assessed by tumor burden in blood measurements (serial CD33+/CD45+ flow cytometry, every 2 weeks) and mice survival. Induction of differentiation was determined by flow cytometry for differentiation markers (CD15, CD11b, CD14) in PB. The levels of 2-HG were determined in collaboration with Lilly researchers.

Treatment with LY3410738 induced earlier and deeper reduction of 2-HG levels after 2 and 4 weeks compared with AG120 (Figure 17).

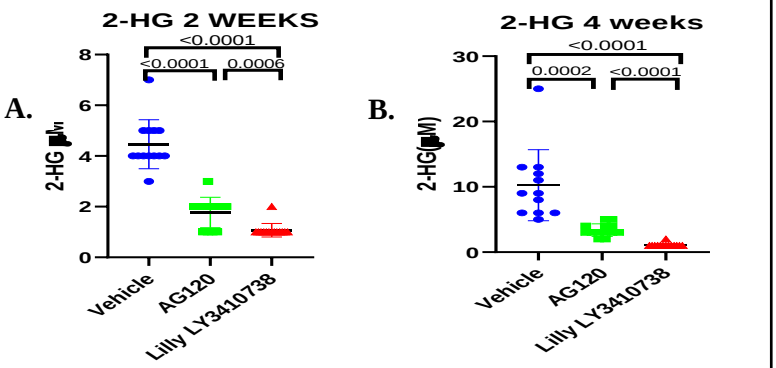

Figure 17: 2-HG level in plasma of AML PDX model with mIDH1 refractory to AG120. **A.** Reduction of 2-HG level after 2 weeks of treatment. **B.** Reduction of 2-HG level after 4 weeks of treatment.

Furthermore, LY3410738 induced significant reduction of the tumor burden in blood detected with reduction of percentages of hCD33+/hCD45+ cells, compared with AG120 (Figure 18A), additionally, it induced myeloid blast cells differentiation into more mature cells through increase in the hCD15+ (Figure 18B) and hCD14+ cells, which was significantly after 4 weeks (Figure 18C). No significant increase in the hCD11b + cells was detected (Figure 18D). No significant change in the survival rate was detected either with AG120 or with LY3410738 treatment due to mice death due to aggressiveness of the PDX model (Figure 19).

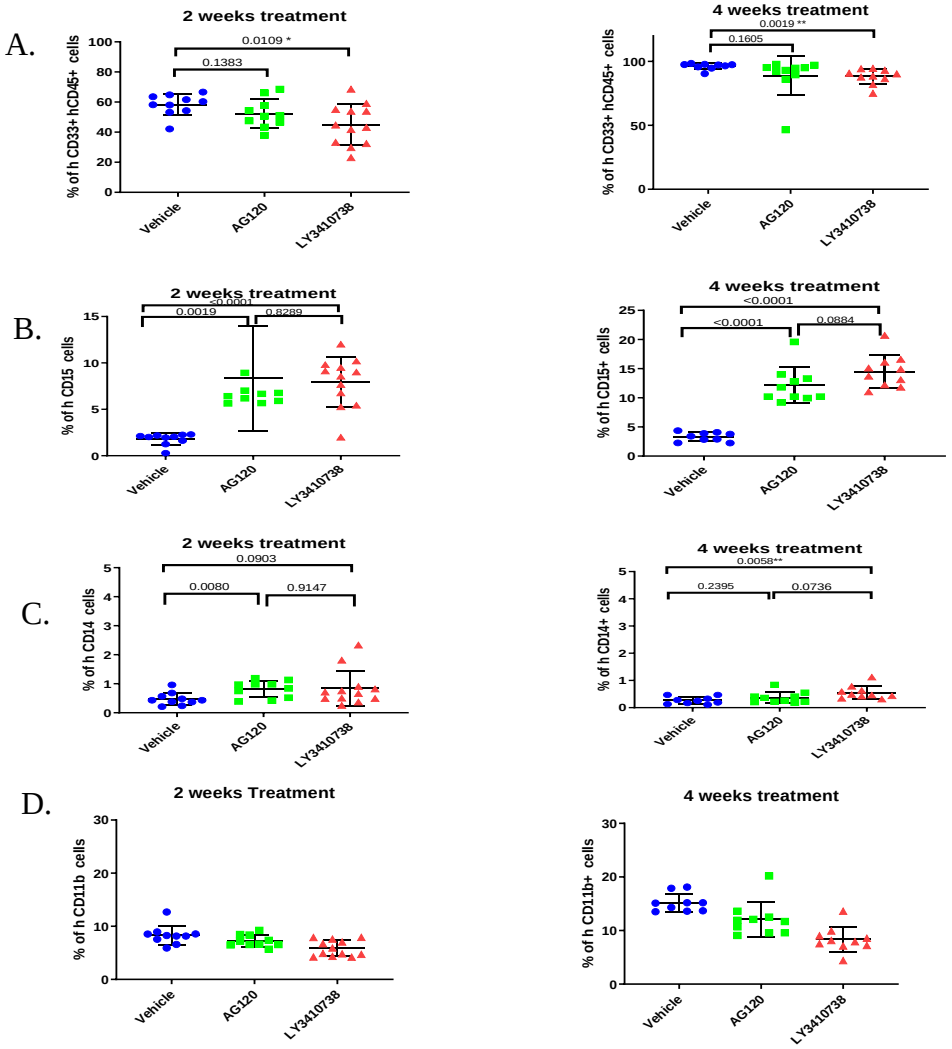

Figure 18: Tumor cells in blood and differentiation markers induced with LY3410738 compared with AG120 in AML PDX model refractory to AG120. A. Tumor burden (CD33+/CD45+). B. CD15 level. C. CD14 level. C. CD11b level

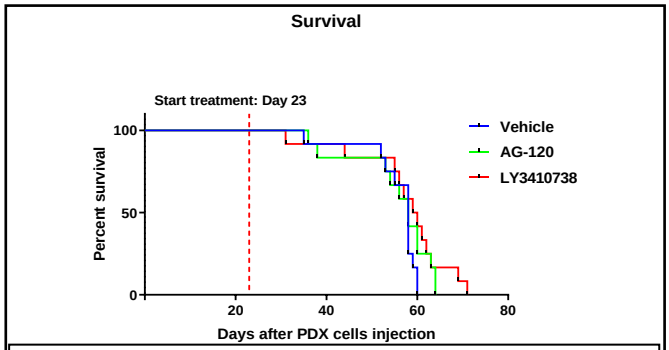

Figure 19: Survival curve of AML PDX model treated with LY3410738 or AG120

Pharmacodynamic Study (PD study) was done after 5 weeks by sacrificing 3 mice from each group (Vehicle, AG120 and LY3410738). Cells were collected from the spleen then human CD45+ (hCD45) cells were sorted by magnetic beads, then the RNA and DNA were extracted for RNA sequencing and DNA methylation essay (Figure 20).

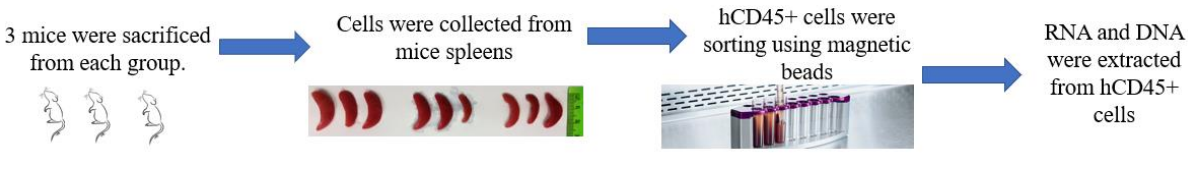

Figure 20: PD Study design of PDX treated with LY3410738 or AG120.

We measured the levels of 2-HG and α-KG in plasma collected from the blood of the sacrificed mice for PD study, which demonstrated significant reduction of the level of 2-HG (Figure 21A) and significant increase in the level of α-KG induced with LY3410738 treatment (Figure 21B).

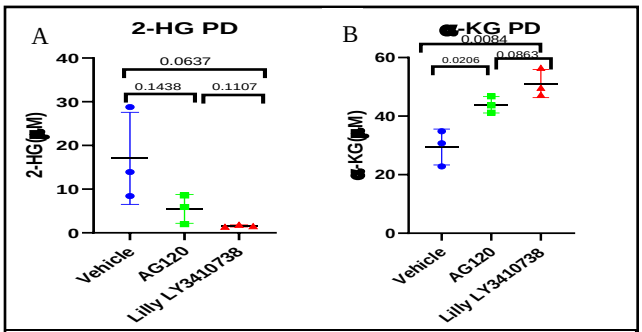

Figure 21: 2-HG and α-KG levels of PD study of AML PDX mice.

Aim 2-b. Changes in gene expression and methylation will be determined through RNAseq analyses and methylation assays.

We performed transcriptomic analysis (RNA seq) of the hCD45+ cells sorted from spleens of mice treated with Vehicle, AG120 and LY2310738 (3 mice per group). Homo Sapiens Human Genome 38 (hg 38) was used as a reference. Samples correlation was studied (Figure 22). Heat Cluster analysis of RNA seq was done (Figure 23).

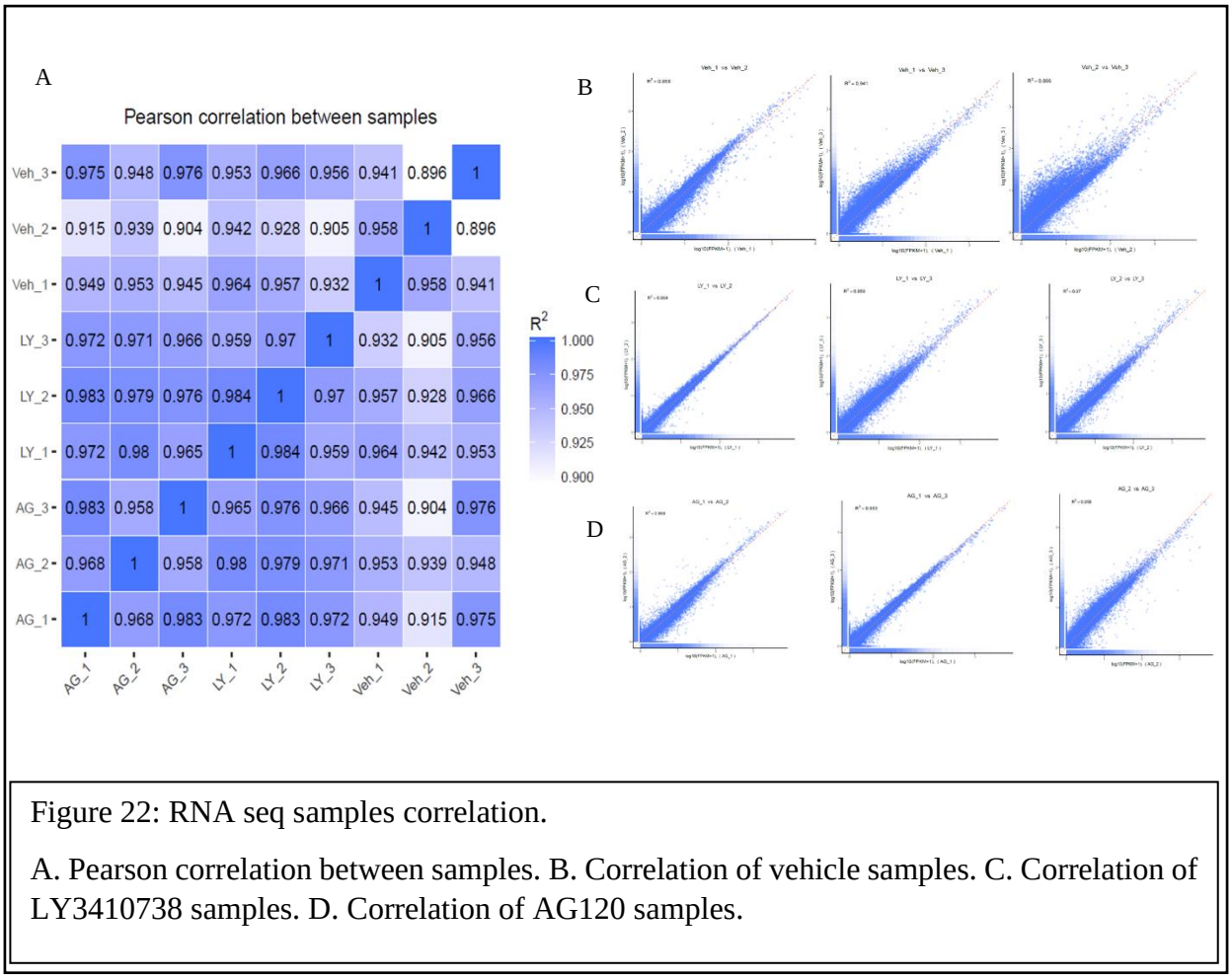

Figure 22: RNA seq samples correlation.

A. Pearson correlation between samples. B. Correlation of vehicle samples. C. Correlation of LY3410738 samples. D. Correlation of AG120 samples.

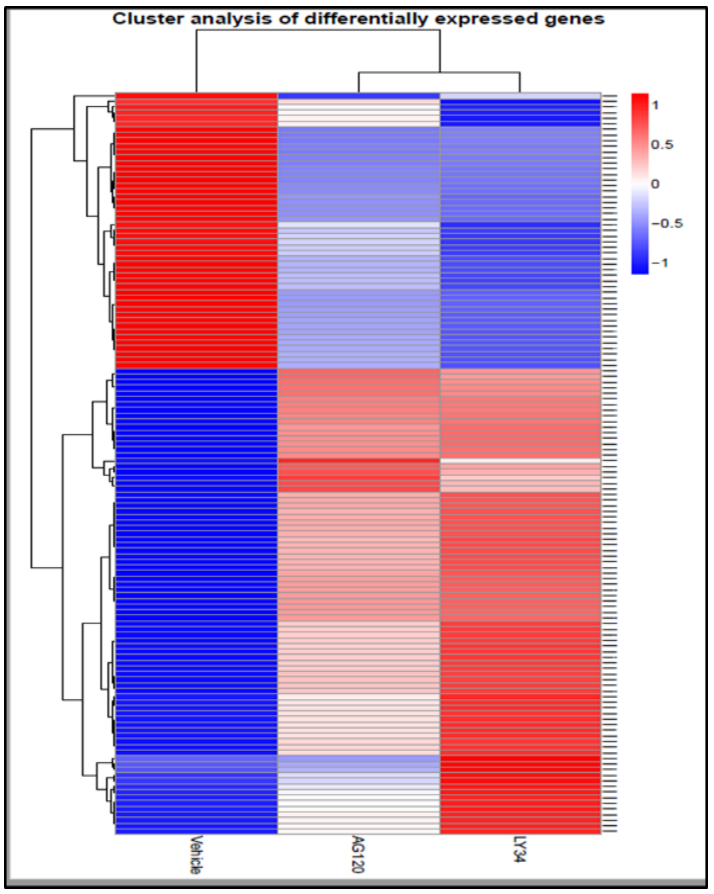

Figure 23: Heat Cluster Analysis of RNA seq of PDX samples (vehicle, AG120 and LY3410738)

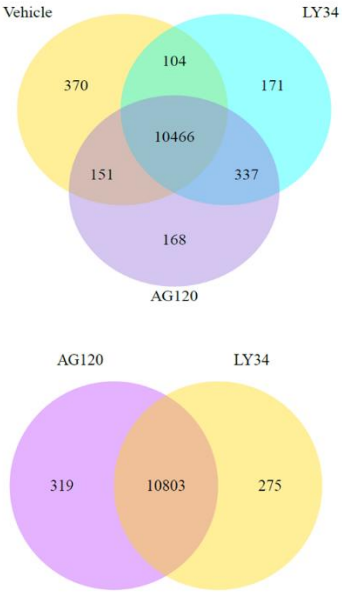

Figure 24: Differential expression analysis of RNA seq of PDX samples.

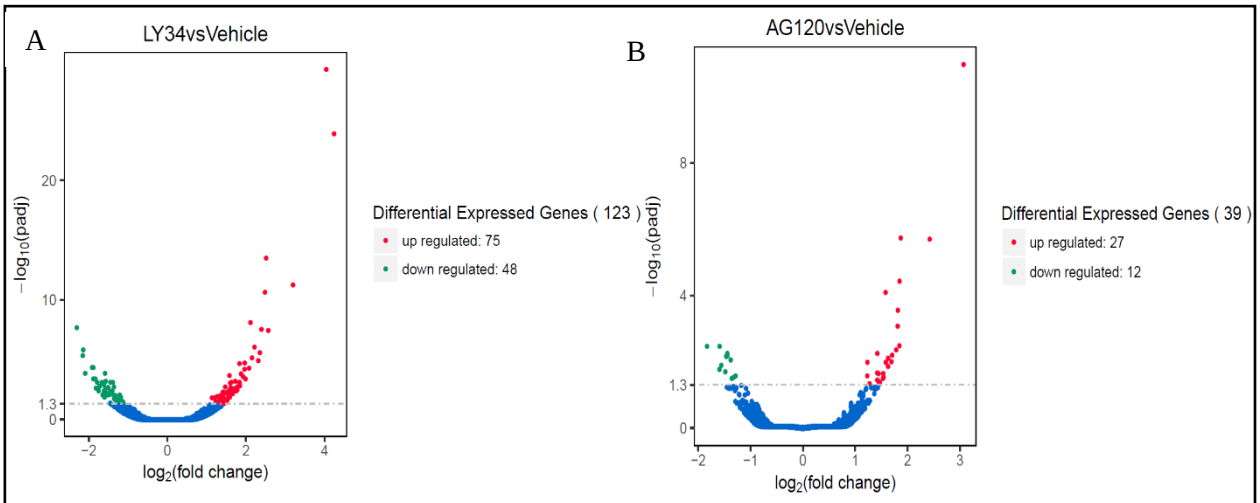

Figure 25: Volcano Differential expression analysis of RNA seq of PDX samples.

A.LY3410738 samples versus Vehicle samples. B. AG120 samples versus Vehicle samples

Upregulated genes induced with LY3410738:

LY3410738 induced upregulation of 75 genes compared with Vehicle (Table 1), it induced myeloid cells activation and differentiation, a strong inflammatory reaction and myeloid and humoral immune response.

Table 1: Upregulated genes induced with LY3410738 compared to Vehicle

GeneName	GeneDescription	log2Fold Change
CLC	Charcot-Leyden_crystal_galectin	4.0438
EREG	epiregulin	4.243
RNASE2	ribonuclease_RNase_A_family_2_(liver_eosinophil-derived_neurotoxin)	2.5156
BPI	bactericidal/permeability-increasing_protein	3.1967
C1orf186	chromosome_1_open_reading_frame_186	2.4844
TRGC2	T_cell_receptor_gamma_constant_2	2.1172
SELP	selectin_P	2.3934
DEFB1	defensin_beta_1	2.5688
RFX8	RFX_family_member_8_lacking_RFX_DNA_binding_domain	2.2179
RHAG	Rh-associated_glycoprotein	2.355
TP53INP2	tumor_protein_p53_inducible_nuclear_protein_2	2.1554
PF4	platelet_factor_4	2.3155
ST8SIA6	ST8_alpha-N-acetyl-neuraminide_alpha-28-sialyltransferase_6	1.9694
MMP15	matrix_metallopeptidase_15	1.8389
ZHX2	zinc_fingers_and_homeoboxes_2	2.0833
UGT3A2	UDP_glycosyltransferase_3_family_polypeptide_A2	1.9644
RP11-354E11.2	NA	1.8759
ATF7IP2	activating_transcription_factor_7_interacting_protein_2	1.5798
IL1RL1	interleukin_1_receptor-like_1	1.9303
FCER1A	Fc_fragment_of_IgE_high_affinity_I_receptor_for;_alpha_polypeptide	1.9941
LYZ	lysozyme	1.73
DAPL1	death_associated_protein_like_1	1.8335
HBD	hemoglobin_subunit_delta	1.8349
LINC00639	long_intergenic_non-protein_coding_RNA_639	1.6302
SERPINE2	serpin_peptidase_inhibitor_clade_E_(nexin_plasminogen_activator_inhibitor_type_1)_member_2	1.6012
HBB	hemoglobin_subunit_beta	1.8456
AGAP7P	ArfGAP_with_GTPase_domain_ankyrin_repeat_and_PH_domain_7_pseudogene	1.7769
ADGRE1	adhesion_G_protein-coupled_receptor_E1	1.4755
HNRNPLL	heterogeneous_nuclear_ribonucleoprotein_L-like	1.615
CYP4F11	cytochrome_P450_family_4_subfamily_F_member_11	1.7171
ST6GALNAC1	ST6_(alpha-N-acetyl-neuraminyl-23-beta-galactosyl-13)-N-acetylgalactosaminide_alpha-26-sialyltransferase_1	1.7614
GOLGA8M	golgin_A8_family_member_M	1.776
RND2	Rho_family_GTPase_2	1.7779
RXFP2	relaxin/insulin-like_family_peptide_receptor_2	1.7669
PPBP	pro-platelet_basic_protein	1.7549
AOAH	acyloxyacyl_hydrolase	1.5637
CTSG	cathepsin_G	1.5611
RP11-84C10.2	NA	1.6439

GeneName	GeneDescription	log2Fold Change
SCD	stearoyl-CoA_desaturase_(delta-9-desaturase)	1.4179
ADRB2	adrenoceptor_beta_2	1.4758
NFE2L3	nuclear_factor_erythroid_2_like_3	1.4298
ST7	suppression_of_tumorigenicity_7	1.6483
PLD1	phospholipase_D1	1.4008
HP	haptoglobin	1.6624
CKM	creatine_kinase_muscle	1.5369
MBOAT2	membrane_bound_O-acyltransferase_domain_containing_2	1.3264
EGR1	early_growth_response_1	1.4034
TRGC1	T_cell_receptor_gamma_constant_1	1.265
TIMP3	TIMP_metallopeptidase_inhibitor_3	1.5888
PIWIL4	piwi-like_RNA-mediated_gene_silencing_4	1.3067
C1orf106	chromosome_1_open_reading_frame_106	1.4197
CCL5	chemokine_(C-C_motif)_ligand_5	1.1371
PLXDC2	plexin_domain_containing_2	1.2036
ASB9	ankyrin_repeat_and_SOCS_box_containing_9	1.5357
CLECL1	C-type_lectin_like_1	1.5195
CNRIP1	cannabinoid_receptor_interacting_protein_1	1.4826
LOXHD1	lipoxygenase_homology_domains_1	1.4815
TRGV10	T_cell_receptor_gamma_variable_10_(non-functional)	1.5271
MAP1LC3A	microtubule_associated_protein_1_light_chain_3_alpha	1.3723
MEX3A	mex-3_RNA_binding_family_member_A	1.3336
HPGDS	hematopoietic_prostaglandin_D_synthase	1.5015
CSGALNACT1	chondroitin_sulfate_N-acetylgalactosaminyltransferase_1	1.3546
CD300LB	CD300_molecule_like_family_member_b	1.4517
GRPEL2	GrpE-like_2_mitochondrial_(E._coli)	1.2288
PLXNB1	plexin_B1	1.4244
CGNL1	cingulin-like_1	1.4819
FAM65C	family_with_sequence_similarity_65_member_C	1.4165
ANO10	anoctamin_10	1.2318
CLTCL1	clathrin_heavy_chain-like_1	1.4689
PRTN3	proteinase_3	1.3981
MTND1P23	mitochondrially_encoded_NADH:ubiquinone_oxidoreductase_core_subunit_1_pseudogene_23	1.3104
CILP2	cartilage_intermediate_layer_protein_2	1.4425
HAL	histidine_ammonia-lyase	1.3869
MS4A7	membrane-spanning_4-domains_subfamily_A_member_7	1.4214
SFRP5	secreted_frizzled-related_protein_5	1.3363

Interestingly, LY3410738 treatment upregulated Lysozyme (LYZ) gene which is a monocyte late differentiation marker (18). Additionally, LY2310738 upregulated Phospholipase D1 (PLD1) which was reported to induce neutrophils activation and AML differentiation into neutrophils through MAPK activation (19). LY3410738 upregulated IL1RL1, which is involved in inflammatory reaction, helper T-cell function and humoral immune response according to NCBI. LY3410738 upregulated Cathepsin G which is a serine protease detected only in cells of myeloid lineage and is expressed within myeloid azurophil granules, it has a rule in host immunity and cleavage of inflammatory mediators and receptors (20).

Enrichment Cluster analysis:

Gene Ontology (GO), Biological Process (BP) analysis revealed upregulation of Granulocytes and Neutrophils activation (myeloid cells activation), humoral immune response (Figure 26A). GO, Molecular Function (MF) analysis revealed upregulation of chemokines receptor binding, chemokine activity, cytokine receptor binding and G-protein coupled receptor binding (Figure 26B). Cellular Compares (CC) analysis revealed upregulation of granule lumen (Figure 26C).

The Human Disease Ontology (DO) revealed upregulation of respiratory system disease, Dermatitis and hypersensitivity reaction diseases. (Figure 26D).

The strong inflammatory response which is possibly associated with induction of myeloid cells differentiation by LY3410738 could also cause a differentiation syndrome, which is a known common side effect of the inducing differentiation drugs as IDH1 inhibitors.

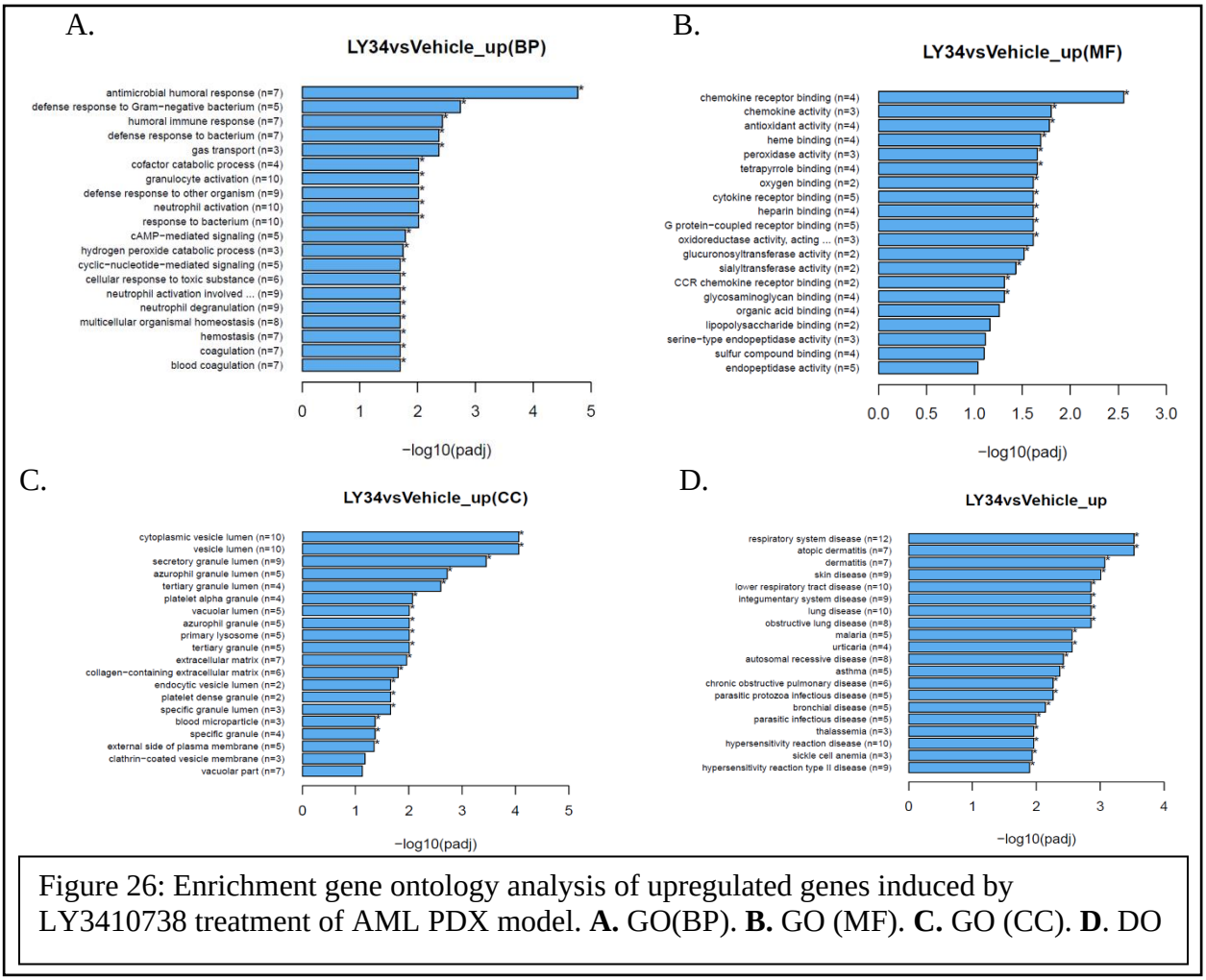

Figure 26: Enrichment gene ontology analysis of upregulated genes induced by LY3410738 treatment of AML PDX model. **A.** GO(BP). **B.** GO (MF). **C.** GO (CC). **D**. DO

Downregulated genes induced with LY3410738:

LY3410738 downregulated 48 genes compared with Vehicle (Table 2). GO (BP) analysis revealed that LY3410738 induced downregulation of; Ras protein signal transduction [CYTH4/DAB2IP/IQSEC1/PLEKHG5/SGK223], phosphatidylinositol 3-kinase signaling (PI3K) [PPP1R16B/PIK3C2B/DAB2IP], and BCR

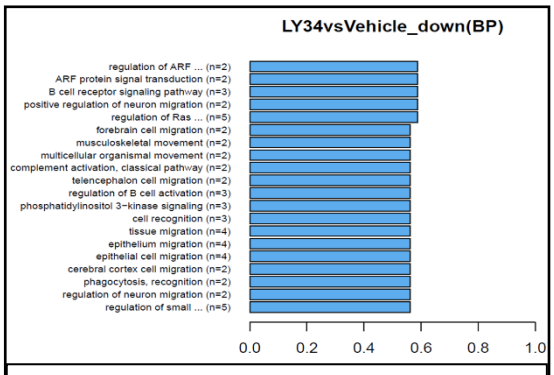

Figure 27: Gene Ontology (BP) of downregulated genes by LY3410738.

signaling pathway [CD22/IGHD/IGHM], inhibition of these pathways may inhibit cell growth.

DO revealed that LY3410738 downregulated AML and ALL [BAALC which is associated with Acute Lymphoblastic Leukemia and Acute Myeloid Leukemia].

Interestingly, LY3410738 downregulated CD7 gene. CD7 is expressed by the leukemic blasts and malignant progenitor cells of approximately 30% of AML patients but is absent on normal myeloid and erythroid cells. CD7 expression by malignant blasts is also linked with chemoresistance and poor outcomes (21).

Abnormal expression or loss of imprinting of H19 has also been correlated with multiple human cancers including hematological malignancies, and associated with poor prognosis (22). LY3410738 also downregulated H19 gene.

Table 2: Downregulated genes induced with LY3410738 compared to Vehicle

Gene Name	GeneDescription	log2Fold Change
PLEKHG5	pleckstrin_homology_and_RhoGEF_domain_containing_G5	-2.3019
MMP28	matrix_metallopeptidase_28	-2.1508
CD7	CD7_molecule	-2.138
CALN1	calneuron_1	-2.0889
MN1	meningioma_(disrupted_in_balanced_translocation)_1	-1.9129
SH3BP5	SH3-domain_binding_protein_5_(BTK-associated)	-1.8829
ZNF467	zinc_finger_protein_467	-1.8817
DNTT	DNA_nucleotidylexotransferase	-1.8323
FLNC	filamin	-1.8176
N4BP3	NEDD4_binding_protein_3	-1.7861
ENAH	enabled_homolog_(Drosophila)	-1.7513
TNNI2	troponin_I_type_2_(skeletal_fast)	-1.7223
BAALC	brain_and_acute_leukemia_cytoplasmic	-1.6645
SOD1P3	superoxide_dismutase_1_soluble_pseudogene_3	-1.6447
ANO9	anoctamin_9	-1.6132
CGREF1	cell_growth_regulator_with_EF-hand_domain_1	-1.6117
LINC00861	long_intergenic_non-protein_coding_RNA_861	-1.5994
CD22	CD22_molecule	-1.5971
SHANK3	SH3_and_multiple_ankyrin_repeat_domains_3	-1.5869
LRRN2	leucine_rich_repeat_neuronal_2	-1.5775
SLC43A2	solute_carrier_family_43_(amino_acid_system_L_transporter)_member_2	-1.5655
CA2	carbonic_anhydrase_II	-1.542
SEMA3A	sema_domain_immunoglobulin_domain_(Ig)_short_basic_domain_secreted_(semaphorin)_3A	-1.5095
KCNK17	potassium_channel_two_pore_domain_subfamily_K_member_17	-1.5063
LTB	lymphotoxin_beta	-1.4803
PPP1R16B	protein_phosphatase_1_regulatory_subunit_16B	-1.4569
KAZALD1	Kazal-type_serine_peptidase_inhibitor_domain_1	-1.4532
VWA1	von_Willebrand_factor_A_domain_containing_1	-1.453
RPS6KL1	ribosomal_protein_S6_kinase_like_1	-1.4503
SH3TC1	SH3_domain_and_tetratricopeptide_repeats_1	-1.4455
IGHD	immunoglobulin_heavy_constant_delta	-1.4081
DAB2IP	DAB2_interacting_protein	-1.4014
PIK3C2B	phosphatidylinositol-4-phosphate_3-kinase_catalytic_subunit_type_2_beta	-1.385
IQSEC1	IQ_motif_and_Sec7_domain_1	-1.359
TNFRSF18	tumor_necrosis_factor_receptor_superfamily_member_18	-1.3528
HIC1	hypermethylated_in_cancer_1	-1.3308
RP4-758J18.10	NA	-1.3285
H19	H19_imprinted_maternally_expressed_transcript_(non-protein_coding)	-1.3278
IGHM	immunoglobulin_heavy_constant_mu	-1.3221
SNED1	sushi_nidogen_and_EGF-like_domains_1	-1.2893
RBPMS	RNA_binding_protein_with_multiple_splicing	-1.285
FCMR	Fc_fragment_of_IgM_receptor	-1.2744
PLEKHA6	pleckstrin_homology_domain_containing_A6	-1.2181
CYTH4	cytohesin_4	-1.2142
MAP1A	microtubule_associated_protein_1A	-1.2052
SGK223	Tyrosine-protein_kinase_SgK223_	-1.192
HLF	hepatic_leukemia_factor	-1.1811
DENND6B	DENN/MADD_domain_containing_6B	-1.1302

Upregulated genes induced with AG120:

AG120 treatment induced upregulation of 27 genes compared with Vehicle (Table 3). Interestingly AG120 upregulated the Lysozyme gene (LYZ) and the myeloid cell nuclear differentiation antigen (MNDA). Both genes induce myeloid cells differentiation and granules formation.

Table 3: Upregulated genes induced with AG120

Gene Name	Gene Description	log2FoldChange
ACSM3	acyl-CoA_synthetase_medium-chain_family_member_3	3.0711
HSD17B6	hydroxysteroid_(17-beta)_dehydrogenase_6	2.4232
TPD52	tumor_protein_D52	1.8711
TP53INP2	tumor_protein_p53_inducible_nuclear_protein_2	1.8472
LYZ	lysozyme	1.8436
BPI	bactericidal/permeability-increasing_protein	1.8148
RHAG	Rh-associated_glycoprotein	1.812
SRGN	serglycin	1.7838
EREG	epiregulin	1.7061
RXFP2	relaxin/insulin-like_family_peptide_receptor_2	1.6932
SERPINE2	serpin_peptidase_inhibitor_clade_E_(nexin_plasminogen_activator_inhibitor_type_1)_member_2	1.6304
HPGDS	hematopoietic_prostaglandin_D_synthase	1.6282
MNDA	myeloid_cell_nuclear_differentiation_antigen	1.5853
GRPEL2	GrpE-like_2_mitochondrial_(E._coli)	1.582
ATF7IP2	activating_transcription_factor_7_interacting_protein_2	1.5436
UGT3A2	UDP_glycosyltransferase_3_family_polypeptide_A2	1.5367
SELP	selectin_P	1.5341
ADGRE1	adhesion_G_protein-coupled_receptor_E1	1.473
ZHX2	zinc_fingers_and_homeoboxes_2	1.4692
SESTD1	SEC14_and_spectrin_domain_containing_1	1.4536
RFX8	RFX_family_member_8_lacking_RFX_DNA_binding_domain	1.4444
TRGC1	T_cell_receptor_gamma_constant_1	1.4226
ANKRD18DP	ankyrin_repeat_domain_18D_pseudogene	1.4226
TRGC2	T_cell_receptor_gamma_constant_2	1.4221
RP11-330A16.1	NA	1.2771
RP11-354E11.2	NA	1.2348
C1orf186	chromosome_1_open_reading_frame_186	1.2306

Downregulated genes induced with AG120

AG120 treatment downregulated 12 genes (Table 4). It downregulated CD7, H19 and DAB2IP founded in the downregulated genes with LY3410738.

Table 4: Downregulated genes induced with AG120 treatment

Gene Name	Gene Description	log2FoldChange
FLNC	filamin_C	-1.8322
H19	H19_imprinted_maternally_expressed_transcript_(non-protein_coding)	-1.3768
DAB2IP	DAB2_interacting_protein	-1.4428
CGREF1	cell_growth_regulator_with_EF-hand_domain_1	-1.5912
SLC43A2	solute_carrier_family_43_(amino_acid_system_L_transporter)_member_2	-1.2854
CD7	CD7_molecule	-1.5578
VWA1	von_Willebrand_factor_A_domain_containing_1	-1.4637
ZNF467	zinc_finger_protein_467	-1.3558
RP4-758J18.10	NA	-1.3164
SHANK3	SH3_and_multiple_ankyrin_repeat_domains_3	-1.4422
MMP28	matrix_metallopeptidase_28	-1.4818
LA16c-312E8.4	NA	-1.5919

In comparison of the upregulated genes induced with LY3410738 compared with the upregulated genes induced with AG120, we noticed that both of them upregulated common genes (Table 5) and downregulated common genes (Table 6). Interestingly we found that LY3410738 upregulated most of the genes that were upregulated with AG120. Additionally, it upregulated extra genes responsible for a strong inflammatory and immune response which were not detected in AG120 samples. LY3410738 treatment Also downregulated almost most of the downregulated genes induced with AG120. According to the found data, IDH1 allosteric inhibitors, induce differentiation through change in the metabolic enzymes; as lysozyme, PLD1 and induces cell maturation through increase in the epiregulin genes. The covalent IDH1 inhibitor (LY3410738) has extra effect on induction of the inflammatory reaction through increase in the cytokines and chemokines formation and binding. It also plays a rule in stimulation of the humoral immune response which is another mechanism of action that can be considered. Both drugs have effect on PI3K and Ras pathways, that can be another mechanism of myeloid blasts death and reduction of the tumor burden.

Mechanistically, upregulation of cytokines binding, chemokines binding was reported to increase the BCL2 dependence (33, 34), which might explain the rational combinatorial anti-leukemia efficacy of the IDH1 inhibitor LY3410738 and BCL2 inhibitor ABT-199 tested in our project. That is why we hypothesized that addition of selective BCL2 inhibitor (ABT-199) to LY3410738 will improve its antileukemic efficacy.

Table 5: Common upregulated genes between LY3410738 and AG120.

Common upregulated genes	Gene Description
TP53INP2	tumor_protein_p53_inducible_nuclear_protein_2
LYZ	lysozyme
BPI	bactericidal/permeability-increasing_protein
RHAG	Rh-associated_glycoprotein
EREG	epiregulin
RXFP2	relaxin/insulin-like_family_peptide_receptor_2
SERPINE2	serpin_peptidase_inhibitor_clade_E_(nexin_plasminogen_activator_inhibitor_type_1)_member_2
HPGDS	hematopoietic_prostaglandin_D_synthase
GRPEL2	GrpE-like_2_mitochondrial_(E._coli)
ATF7IP2	activating_transcription_factor_7_interacting_protein_2
UGT3A2	UDP_glycosyltransferase_3_family_polypeptide_A2
SELP	selectin_P
ADGRE1	adhesion_G_protein-coupled_receptor_E1
ZHX2	zinc_fingers_and_homeoboxes_2
RFX8	RFX_family_member_8_lacking_RFX_DNA_binding_domain
TRGC1	T_cell_receptor_gamma_constant_1
TRGC2	T_cell_receptor_gamma_constant_2
RP11-354E11.2	NA

Table 6: Common downregulated genes between LY3410738 and AG120

Common Downregulated genes	Gene Description
FLNC	filamin_C
H19	H19_imprinted_maternally_expressed_transcript_(non-protein_coding)
DAB2IP	DAB2_interacting_protein
CGREF1	cell_growth_regulator_with_EF-hand_domain_1
SLC43A2	solute_carrier_family_43_(amino_acid_system_L_transporter)_member_2
CD7	CD7_molecule
VWA1	von_Willebrand_factor_A_domain_containing_1
ZNF467	zinc_finger_protein_467
RP4-758J18.10	NA
SHANK3	SH3_and_multiple_ankyrin_repeat_domains_3
MMP28	matrix_metallopeptidase_28

DNA Methylation Assay

LY3410738 didn't show a significant effect on DNA methylation compared with AG120:

DNA extracted from hCD45+ cells sorted from cells collected from spleens of mice, were sent to the Epic Microarray core facility, MD Anderson Cancer center for DNA methylation assay. Data was analyzed using specific cluster analysis. We didn't find significant difference in the mean beta values of DNA methylation of CPGs induced with LY3410738 or AG120 compared to vehicle, in all analyzed sites of DNA (All, Island, non-promotor, promotor, Shelf, Shore, Opensea) (Figure 28).

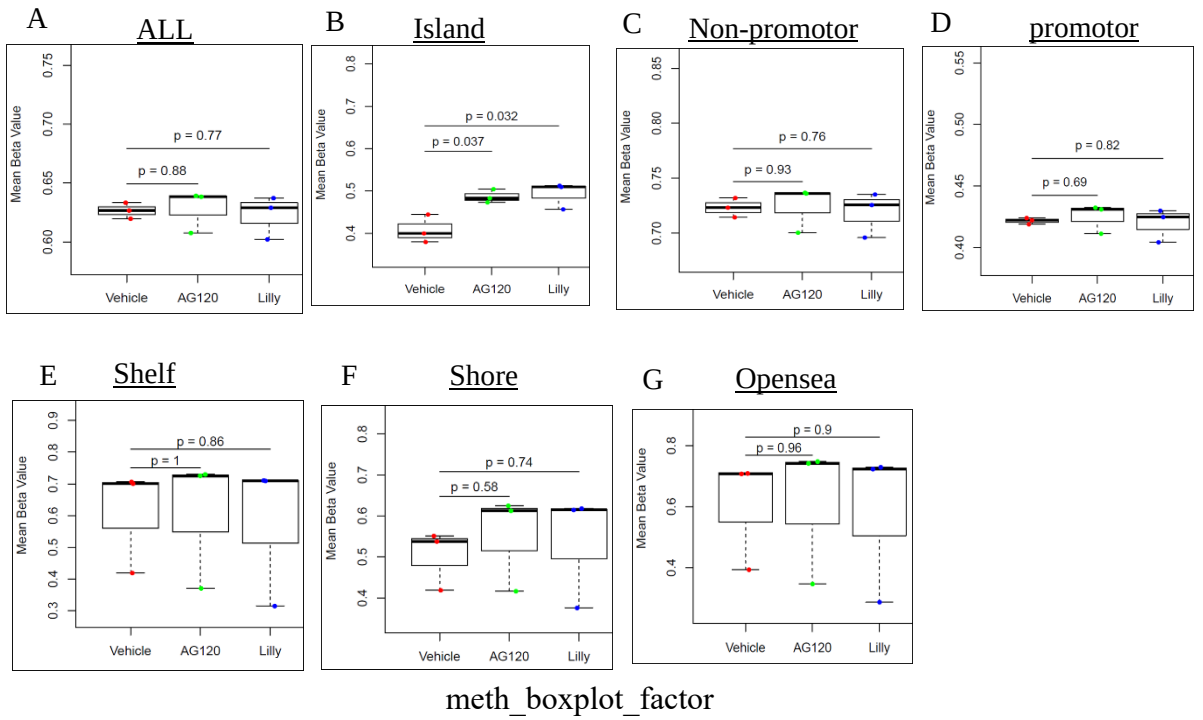

Figure 28: DNA methylation analysis. Mean beta value of top 1% most variable CpGs of each group (Vehicle, AG120 or LY3410738). Different methylation CpG islands (sites) were studied, A. All site of genes. B. Island. C. Non-promotor. D. Promotor. E. Shelf. F. Shore. G. Opensea.

We compared the hypomethylated genes induced with LY3410738 with the upregulated genes induced with that agent detected in RNA seq. Interestingly we noticed some upregulated genes detected in the RNA seq analysis were DNA hypomethylated in DNA methylation analysis. The common genes were plotted (Table 7).

Table 7: common hypomethylated and upregulated genes induced with LY3410738

Probe (CpG)	Gene	cgi	logFC
cg19930657	PLD1	shore	0.458822
cg20060108	IL1RL1	opensea	0.332663
cg24777950	CTSG	opensea	0.313459
cg20543211	PPBP	opensea	0.286025
cg01697902	CTSG	opensea	0.284432
cg16798878	CTSG	opensea	0.213093
cg26810323	IL1RL1	opensea	0.197414
cg13009654	EGR1	island	0.194273
cg15863841	PLD1	opensea	0.169403
cg14513570	DAPL1	opensea	0.153271

Aim 3a: To test the rationale combination of the novel IDH1 inhibitor with targeted agent BCL-2 selective antagonist ABT199 in PDX model In vivo:

Combining LY3410738 with ABT-199 improved its antileukemic effect in AML PDX model refractory to AG120.

PDX model has been established with IDH1-mutant AML (FLT3-ITD, DNMT3A, **IDH1/R132H**, KIT, NPM1) refractory to AG120 (PDX #1). We used 8-9 mice/group. Engrafted mice were orally gavaged with either; Vehicle, 10mg/kg LY3410738 once daily (including the weekends), 50mg/kg ABT-199 once daily for continuous 2 weeks (including the weekends) and one week off or combination of 10mg/kg LY3410738 + 50mg/kg ABT-199. The anti-leukemia activity was assessed by tumor burden measurements (serial CD33+/CD45+ flow cytometry, every 2 weeks) and mice survival. Induction of differentiation was determined by flow cytometry using differentiation markers (CD11b, CD14 and CD15) in PB.

Measuring the level of 2-HG in the plasma of treated mice after 2, 4 and 6 weeks of treatment, showed that LY3410738 significantly decreased the level of 2-HG as a single drug and in the combination with ABT-199. Interestingly that ABT-199 treated mice showed also decrease in the level of 2-HG due to reduction of the tumor burden (Figure 29).

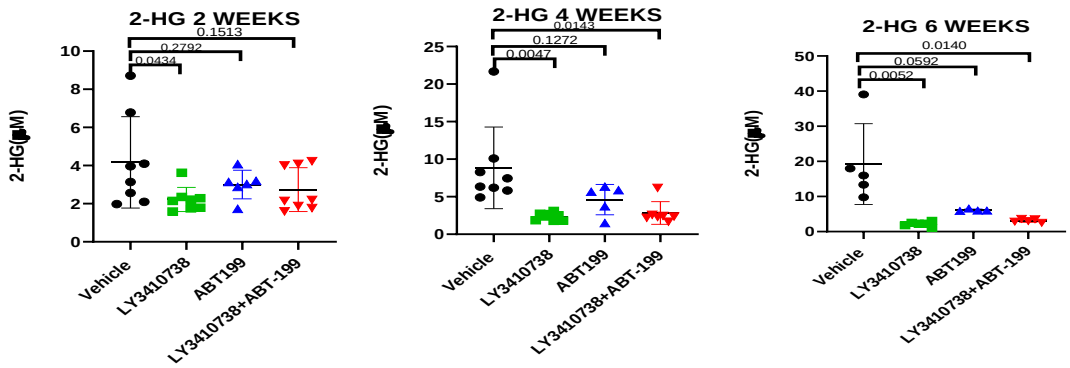

Figure 29: 2-HG levels in plasma of mice of PDX #1 of the combination study (LY3410738 + ABT-199). A. 2-HG level after 2 weeks. B. 2-HG levels after 4 weeks. C. 2-HG after 6 weeks of treatment

Measuring the level of α-KG, revealed that LY3410738 has no significant effect on α-KG. Interestingly, ABT-199 as a single agent and the combination LY3410738 and ABT-199, induced significant increase in α-KG after 6 weeks of treatment, most probably due to reduction of AML blast cells (Figure 30).

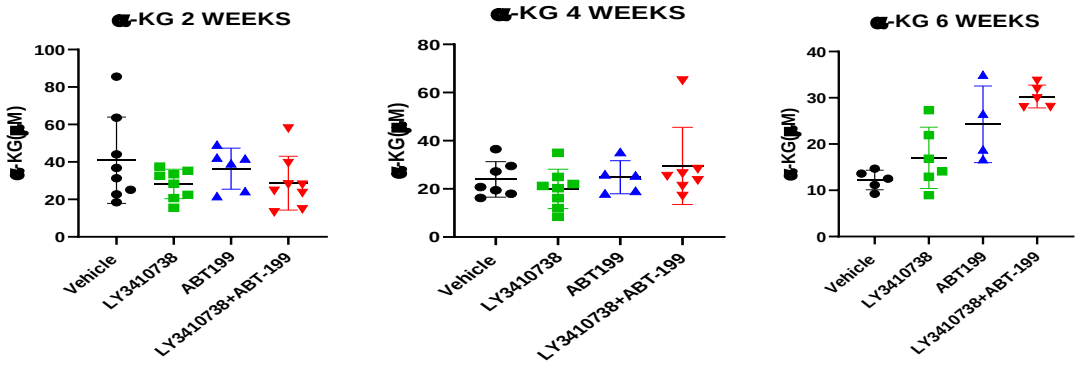

Figure 30: α-KG levels in plasma of mice of PDX #1 of the combination study (LY3410738 + ABT-199).

A. 2-HG level after 2 weeks with no Signiant difference. B. 2-HG levels after 4 weeks with no significant difference. C. 2-HG after 6 weeks of treatment showed that there is significant increase induced with AB-199 and the Combination therapy (LY3410738 + ABT-199).

Combining LY3410738 with ABT-199 translated into additive reduction of the tumor burden detected by percentage of hCD33+/hCD45+ cells (Figure 31), no significant difference noted in the survival rate curve (Figure 32).

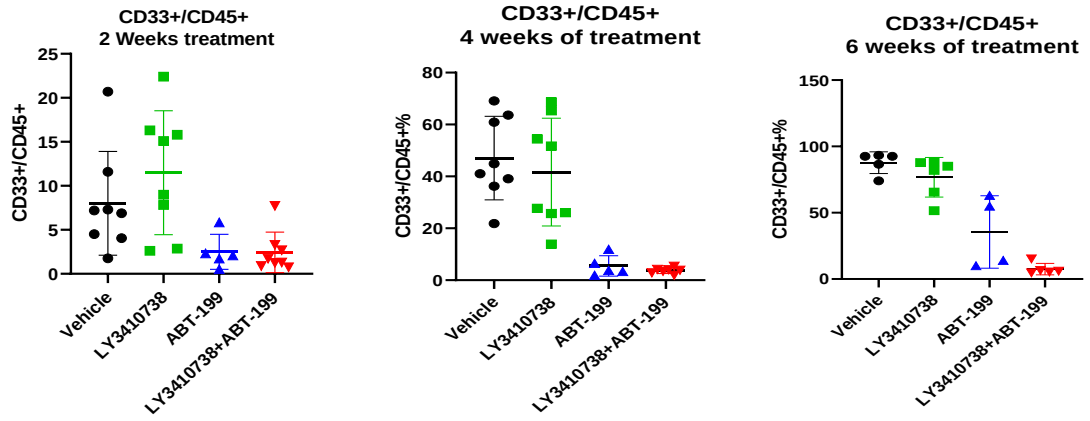

Figure 31: Reduction of tumor burden in blood with Combination therapy of LY3410738 and ABT-199 in PDX #1.

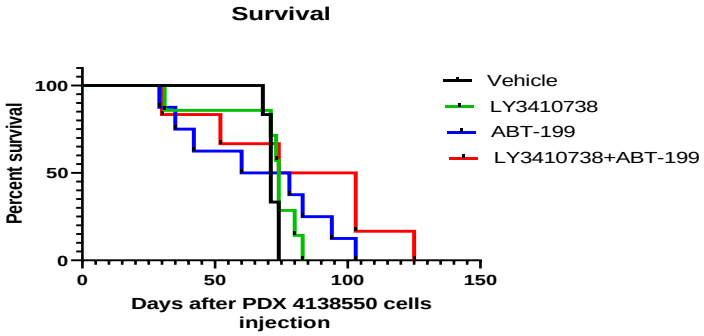

Figure 32: Survival curve of the combination therapy in PDX#1

Moreover, LY3410738 induced differentiation of AML, measurable by increase in the percentages of hCD15+ and hCD14+. Surprisingly, ABT-199 induced increase in the

percentage of differentiation markers hCD15 and hCD14 after 2 weeks of therapy, followed by subsequent reduction with continued treatment.

Combining LY3410738 with ABT-199 facilitated differentiation by increasing the percentage of hCD15 (Figure: 33A) and hCD14 (Figure: 33B) after 2 and 4 weeks of treatment. No significant effects on the percentage of CD11b were noted (Figure: 33C).

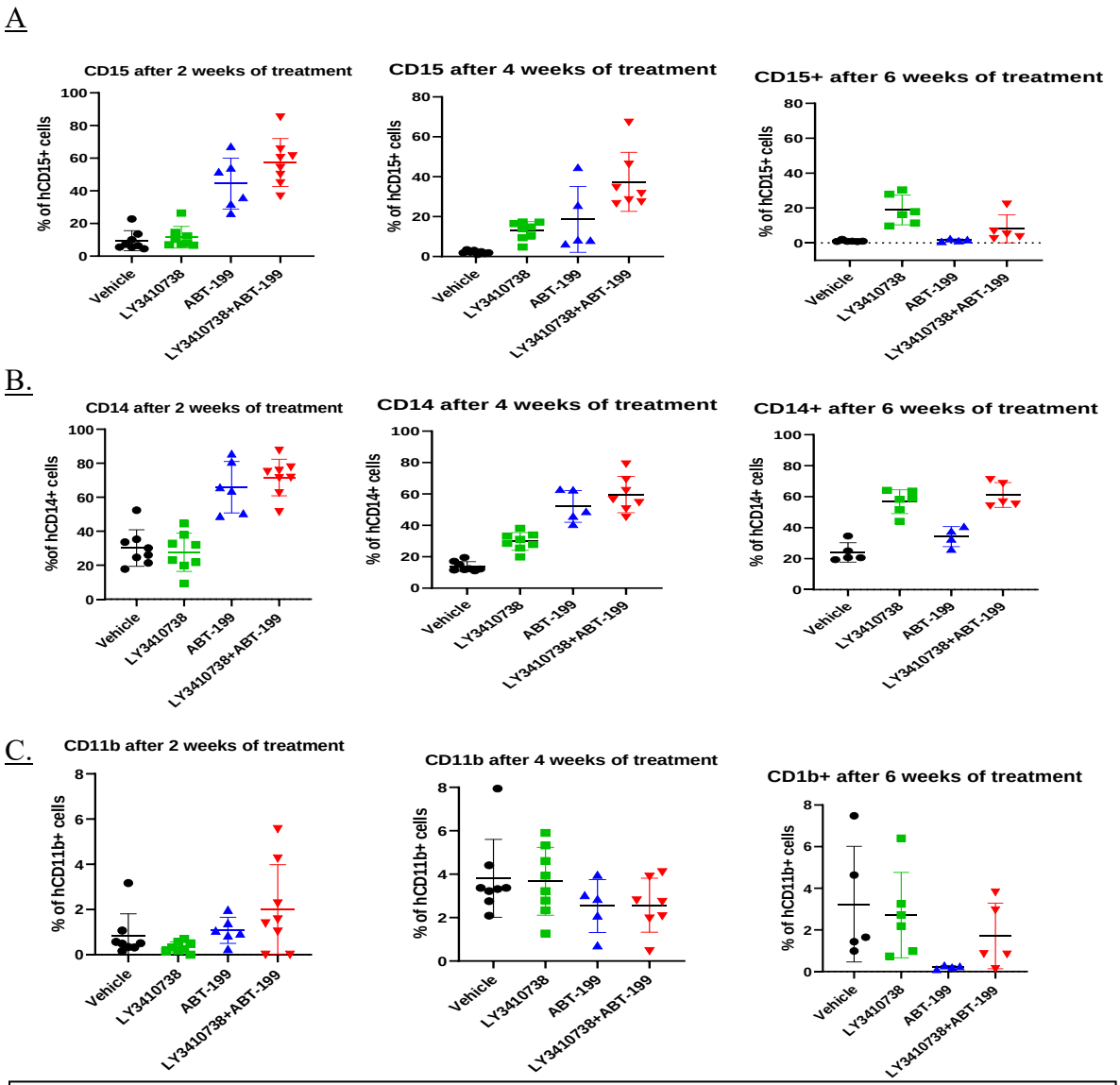

Figure 33: Differentiation markers of PDX #1 of combination study.

A.CD15 marker after 2, 4 and 6 weeks. B. CD14 marker after 2, 4 and 6 weeks. C. CD11b marker after 2, 4 and 6 weeks.

Pharmacodynamic Studies (PD Study):

Pharmacodynamic studies (PD study) after 5 weeks of therapy were done by sacrificing 2 mice from Vehicle, LY3410738 and the combination groups. We didn't sacrifice mice from the ABT-199 group due to small cohort number due to death of mice due to ABT-199 side effects. Blood was collected from mice and plasma was extracted to measure the 2-HG and α-KG levels. Cells were collected from spleens and Bone Marrow (BM) for cell counting and flowcytometry. hCD45+ cells were sorted from cells collected from spleen for DNA extraction for DNA methylation assay (Figure 34).

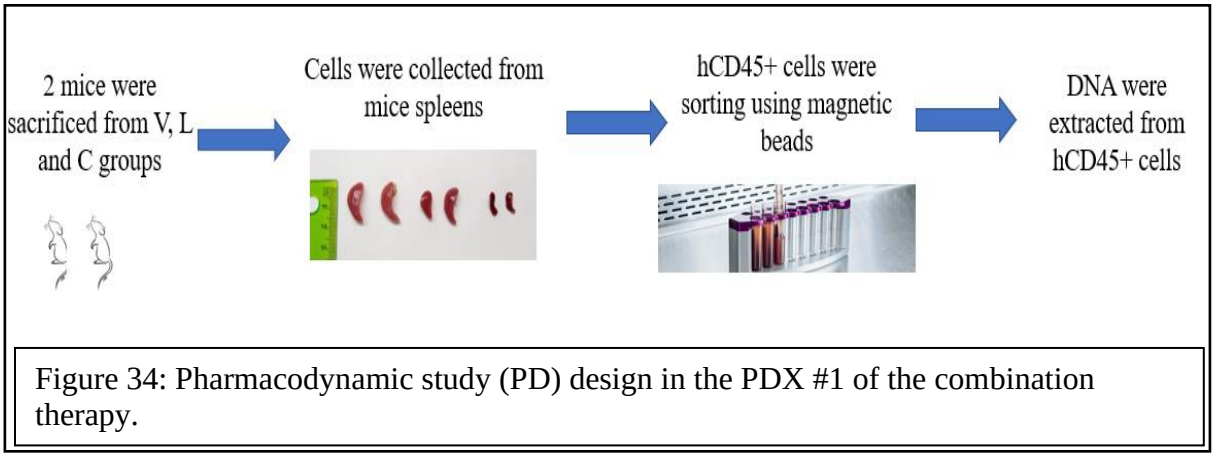

Figure 34: Pharmacodynamic study (PD) design in the PDX #1 of the combination therapy.

Additive decrease in the size and weight of the spleen in the mice treated with the combination therapy (LY3410738 and ABT-199) compared to mice treated with the Vehicle or with LY3410738 alone (Figure 35).

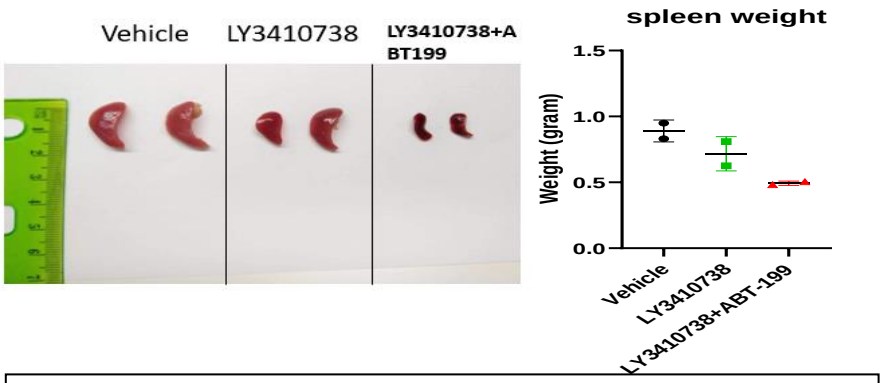

Figure 35: Spleen size and weight of PD study of PDX #1 in the combination therapy

Measuring the levels of 2-HG showed significant decrease with LY3410738 treatment as a single agent and with the combination therapy, but no significant difference between LY3410738 as a single agent and in combination with ABT-199 (Figure 36 A). No significant effect on the level of α-KG was detected either with LY3410738 alone or in combination with ABT-199 Figure 36B).

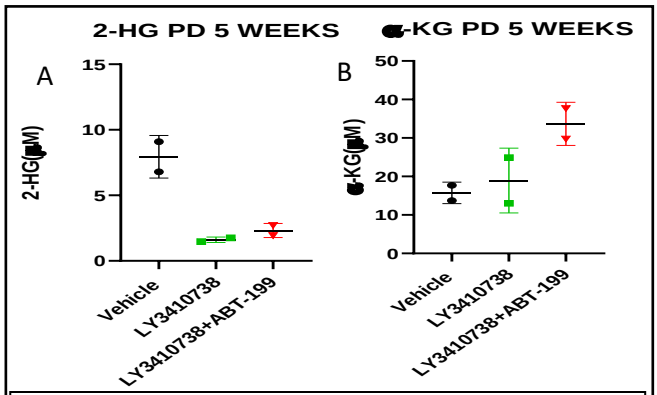

Figure 36: 2-HG and α-KG levels in plasma of PDX#1 mice of the combination therapy.

Counting the viable cells collected from the spleen and BM with trypan blue demonstrated decrease in the number of the cells and the number of the hCD45, after magnetic sorting, from the spleen of the mice treated with the combination therapy (Figure 37).

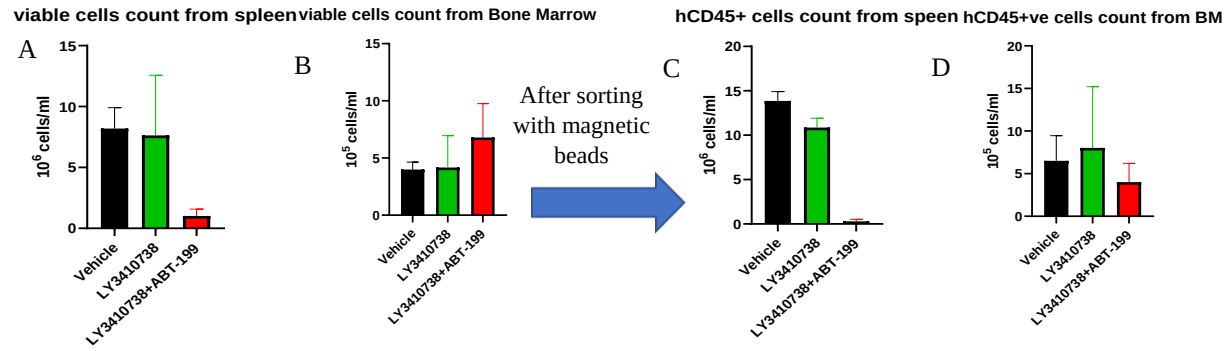

Figure 37: Spleen and BM cells counting before and after sorting with magnetic beads, PD study of PDX #1 of the combination study.

A.Spleens cell count before sorting. B. BM cell count before sorting. C. Spleens cell count after sorting. D. BM cell count after sorting.

Flowcytometry:

Flowcytometry analysis of cells collected from blood, spleen and BM was done. Further decrease in AML tumor burden (detected by the percentage of hCD33+/hCD45+) was detected in the PB, spleen and BM in the mice treated with the combination therapy compared to LY3410738 alone (Figure 38). More increased fraction of differentiated populations (increase in the percentage of hCD15 (Figure 39A) and hCD14 (Figure 39B)) in the mice treated with the combination therapy, except in BM, we detected reduction of the percentage of hCD15. No significant increase in the level of hCD11b was detected either in blood, spleen or BM (Figure 39C).

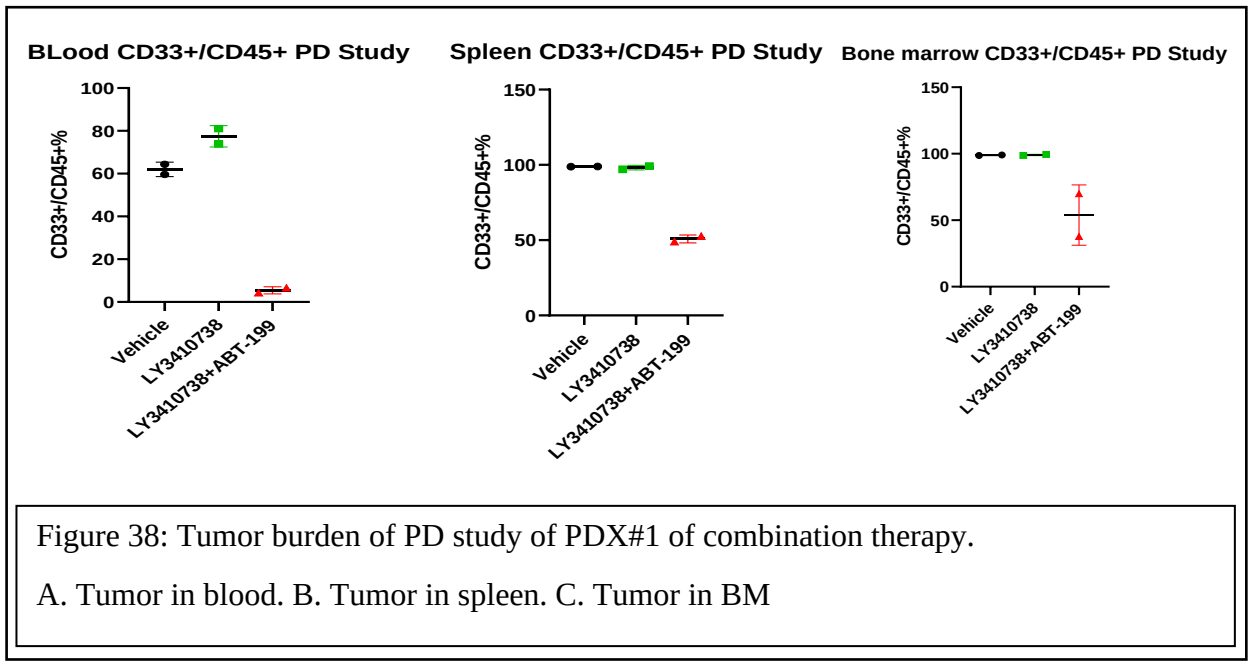

Figure 38: Tumor burden of PD study of PDX#1 of combination therapy.

A. Tumor in blood. B. Tumor in spleen. C. Tumor in BM

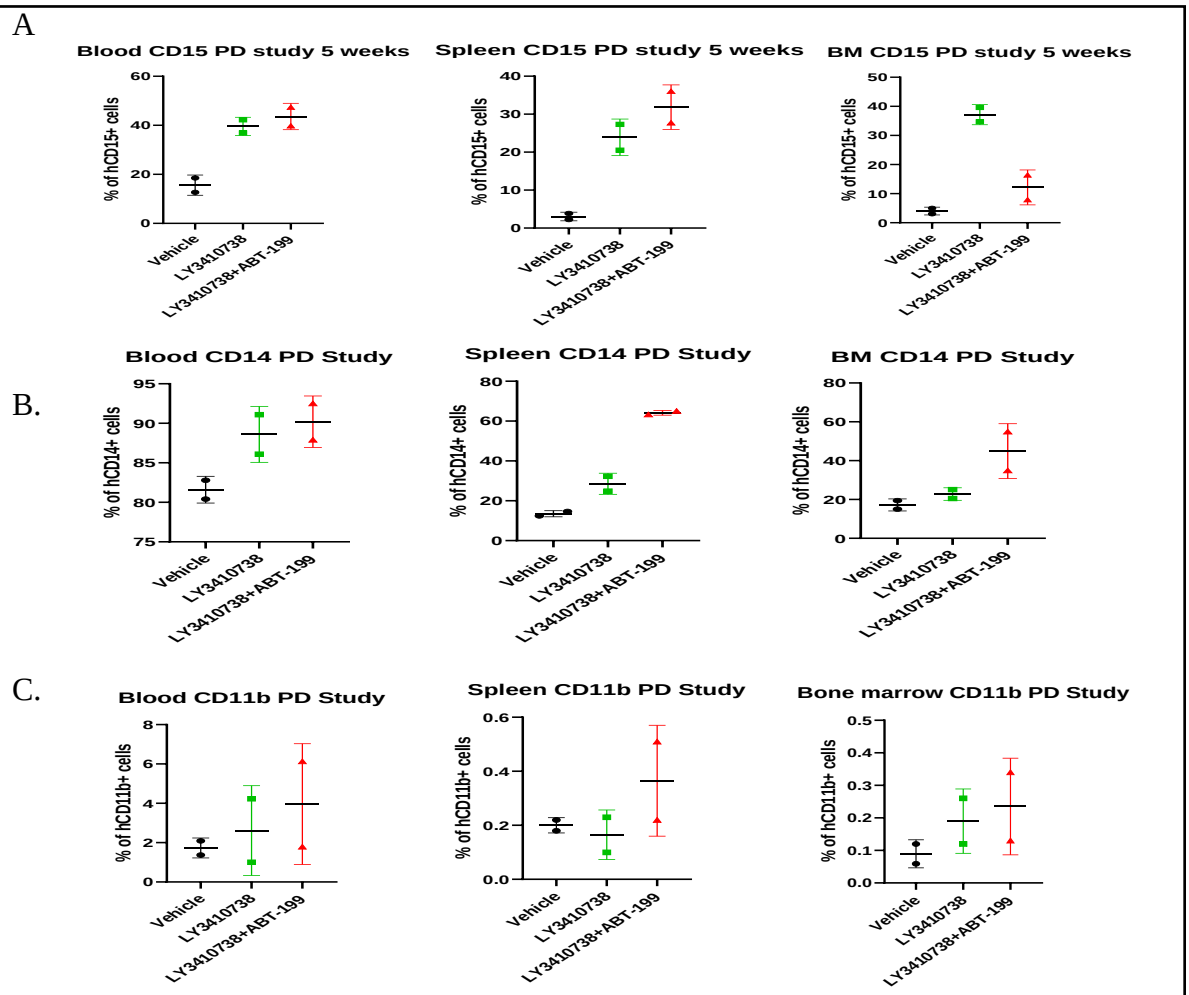

Figure 39: Differentiation markers in PD study of PDX#1 of the combination therapy study. A.

DNA Methylation:

DNA extracted from hCD45+ cells sorted from cells which were collected from spleens of mice, were sent to the Epic Microarray core facility, MD Anderson Cancer center for DNA methylation assay. Data was analyzed using specific cluster analysis. Only significant decrease in the mean beta value of DNA methylation (compared with vehicle) was detected by LY3410738 (of top 1% most variable CpGs for each sample) in the shelf, shore and opensea sites. Global DNA hypermethylation was detected in the combination therapy (Figure 40). Interesting hypomethylated genes induces with LY3410738 was plotted (Table 8).

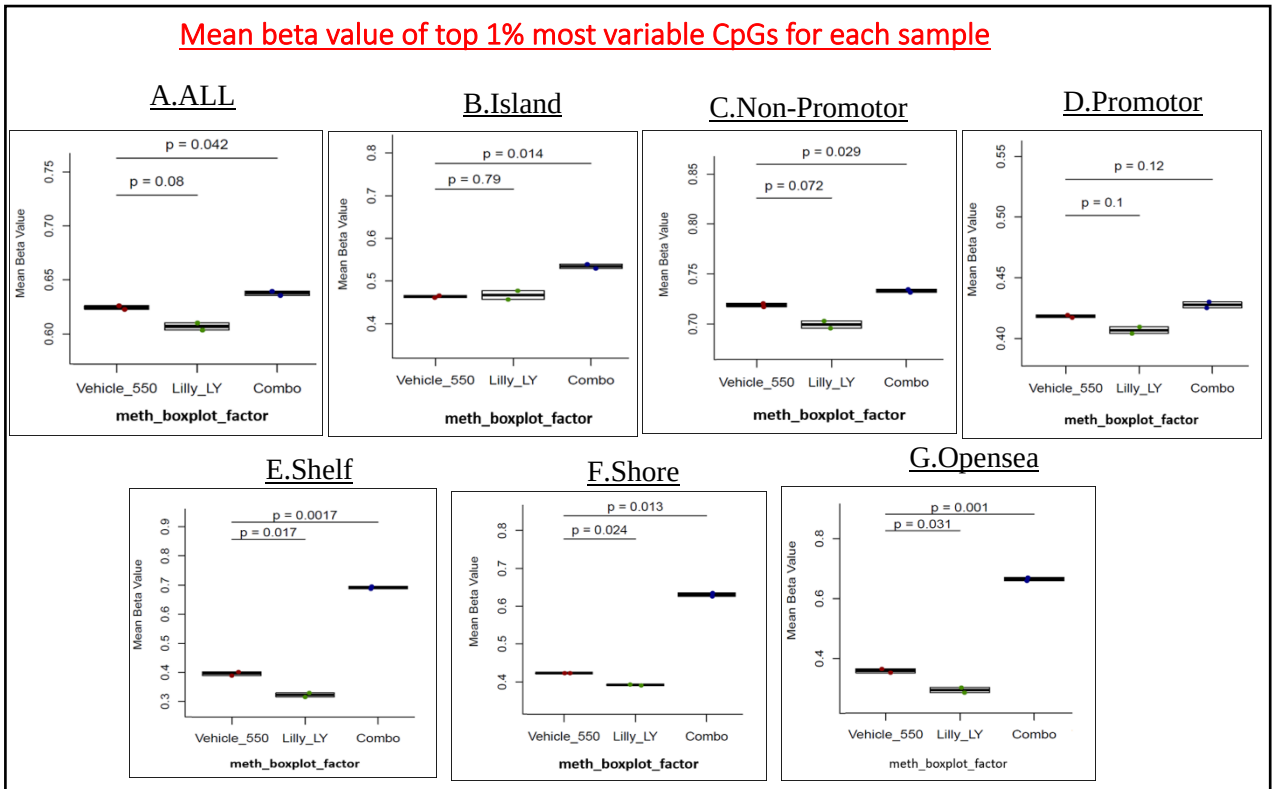

Figure 40: DNA methylation analysis. Mean beta value of top 1% most variable CpGs of each group (Vehicle, AG120 or LY3410738). Different methylation CpG islands (sites) were studied, A. All site of genes. B. Island. C. Non-promotor. D. Promotor. E. Shelf. F. Shore. G. Opensea.

Table 8: Interesting hypomethylated genes induced with LY3410738

Probe	gene	cgi	adj.P.Val	logFC
cg11543559	IL1R1	opensea	0.01443955	0.647811
cg19930657	PLD1	shore	0.01443955	0.61948
cg03272225	JAK3	shore	0.01443955	0.613928
cg27624466	MAP3K7	opensea	0.01443955	0.586839
cg01385762	MAP3K1	opensea	0.01443955	0.566429
cg18442793	IL10	opensea	0.01443955	0.484572
cg26810323	IL1RL1	opensea	0.01443955	0.47853
cg06584121	IL13	shore	0.01443955	0.424339
cg20593471	BCL2	opensea	0.01443955	0.41219
cg24264287	IL6R	opensea	0.01502702	0.404717
cg25783189	FGR	opensea	0.01443955	0.365377
cg25194937	PPBP	opensea	0.01545984	0.349202
cg02867514	CCL5	opensea	0.02593645	0.320179
cg11189107	CTSG	opensea	0.04328719	0.158272
cg23560546	DAPL1	opensea	0.05863611	0.15582

Testing the combination of the novel IDH1 inhibitor with targeted agent BCL-2 selective antagonist ABT199 in another PDX model In vivo (PDX model #2):

Combining LY3410738 with ABT-199 improved its antileukemic effect in AML PDX model #2.

PDX model #2 has been established with IDH1-mutant AML (FLT3-ITD, DNMT3A, IDH1/R132, KIT, NPM1) not treated with AG120. 12 mice per group were used. Engrafted mice were orally gavaged with either; Vehicle, 10mg/kg LY3410738 once daily (including the weekends), 50mg/kg ABT-199 once daily for continuous 2 weeks (including the weekends) and one week off or combination of 10mg/kg LY3410738 + 50mg/kg ABT-199. The anti-leukemia activity was assessed by tumor burden measurements in PB (serial CD33+/CD45+ flow cytometry, every 2 weeks) and mice survival. LY3410738 decreased the tumor burden significantly after 6 weeks of treatment. Combining LY3410738 with ABT-199 translated into additive reduction of the tumor burden detected by hCD33+/CD45+, but no significant difference between the combination therapy and the ABT-199 as a single agent (Figure 41).

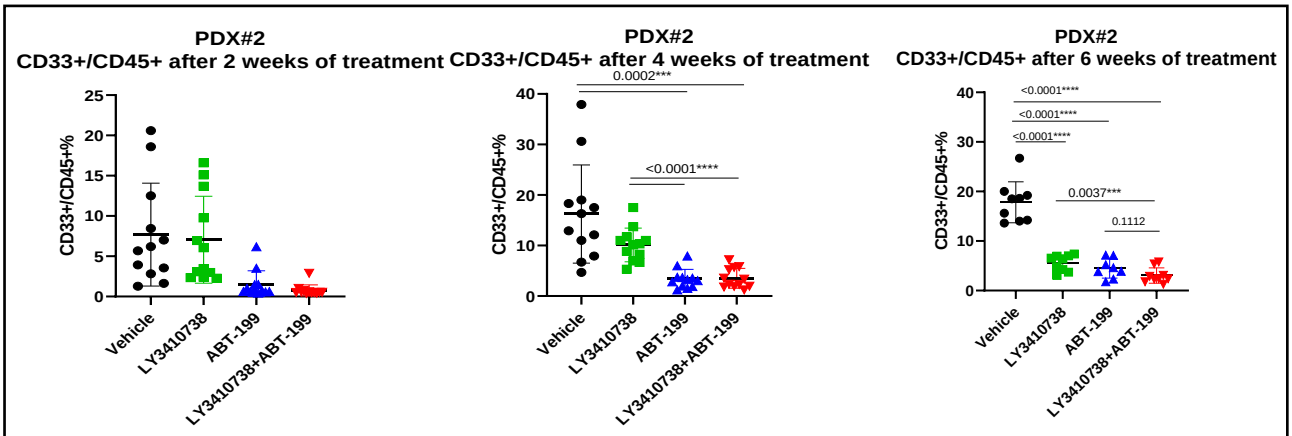

Figure 41: Tumor burden in blood of PDX #2 in combination study

Induction of differentiation was determined by flow cytometry using differentiation markers (hCD11b, hCD14 and hCD15) in PB. LY3410738 gradually induced differentiation

of AML, measurable by increase in the percentage of hCD15+, interestingly ABT-199 induced increase in hCD15+ and hCD14+ cells in the first 4 weeks followed by subsequent reduction with continued treatment. Combining LY3410738 with ABT-199 facilitated differentiation by increasing the percentage of hCD15+ (Figure 42A) and hCD14+ (Figure 42B) after 2 and 4 weeks of treatment. No significant effects on CD11b were noted (Figure 42C).

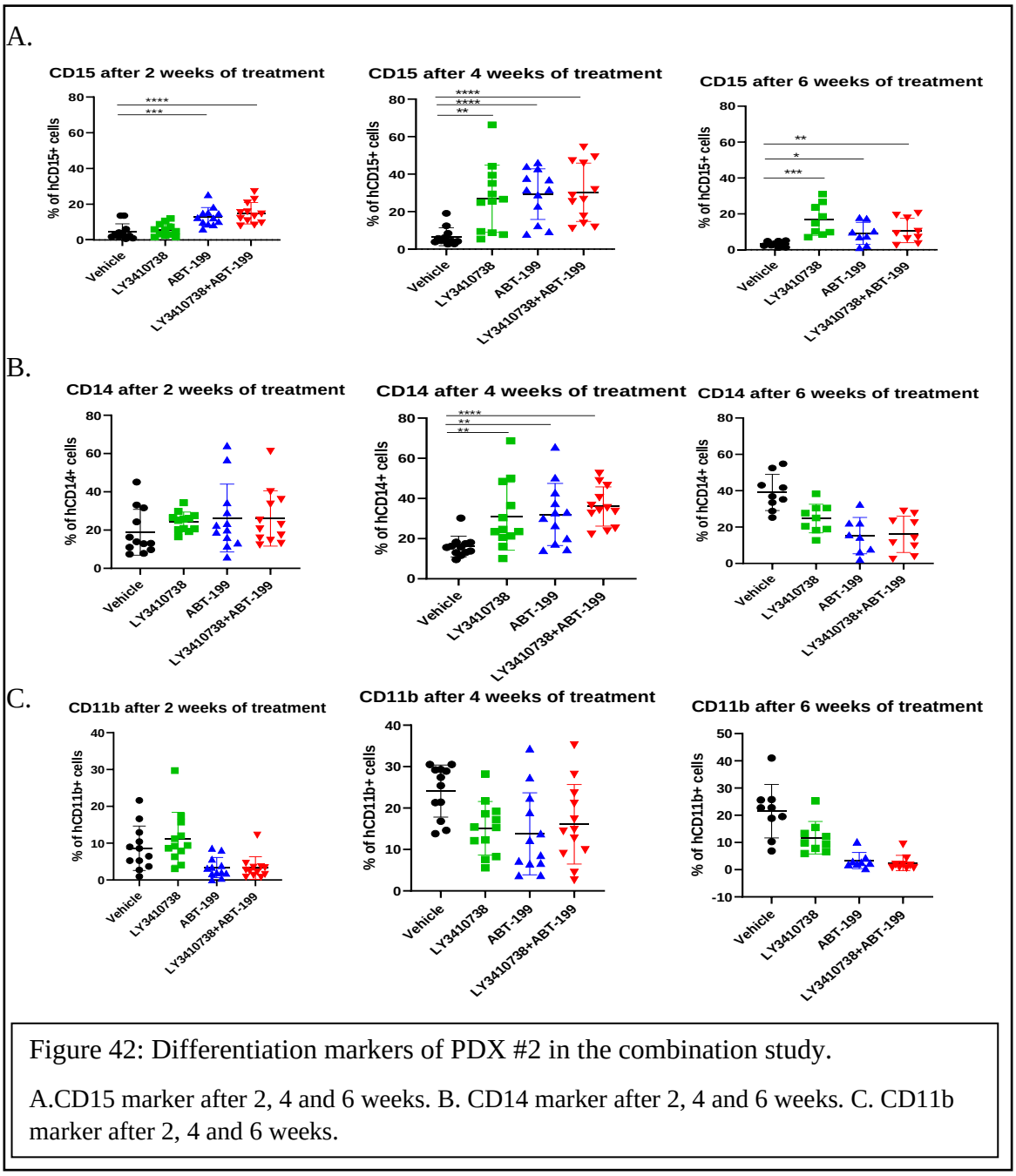

Figure 42: Differentiation markers of PDX #2 in the combination study.

A.CD15 marker after 2, 4 and 6 weeks. B. CD14 marker after 2, 4 and 6 weeks. C. CD11b marker after 2, 4 and 6 weeks.

To study the effect of the treatment with LY3410738 as a single agent or in combination with ABT-199 on the myeloid leukemia primitive cells we used hCD117 marker, which demonstrated that LY3410738 increased in the percentage of hCD117+ marker after 2 weeks of treatment due to induction of differentiation then followed by reduction of the hCD117+ cells significantly after 6 weeks of treatment. Combining LY3410738 with ABT-199 translated into additive reduction of myeloid primitive cells detected by hCD117+ but no significant difference between the combination therapy and ABT-199 alone was detected (Figure 43).

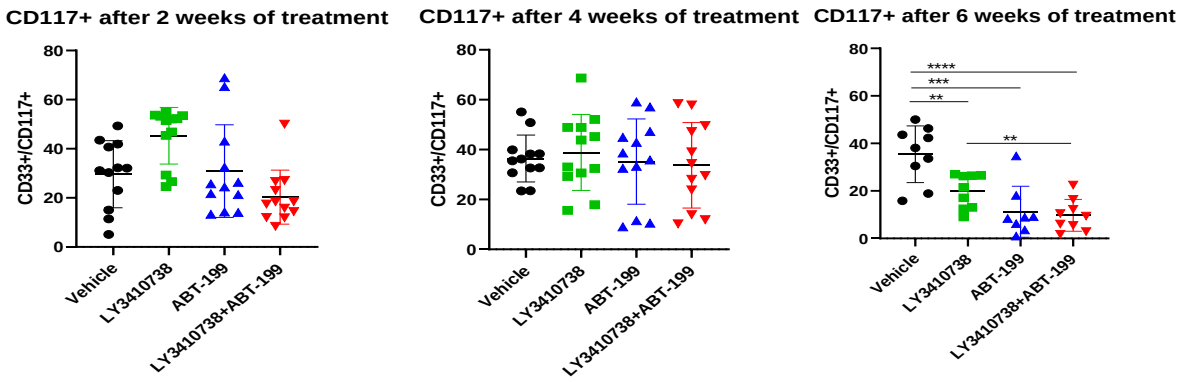

Figure 43: Myeloid Leukemia primitive cell marker hCD177 in PDX #2 of the combination study

Pharmacodynamic Studies (PD Studies):

PD studies after 5 weeks of therapy were done by sacrificing 3 mice from each group (Vehicle, LY3410738, ABT-199 and Combination therapy). Blood was collected from mice by eye bleeding for plasma extraction to measure the 2-HG and α-KG levels. Cells were collected from spleens and Bone Marrow (BM) for cell counting and flowcytometry. Human CD45+ cells were sorted from cells collected from spleen for RNA extraction needed for RNA sequencing analysis.

Additive decrease in the size and weight of the spleen in the mice treated with the combination therapy (LY3410738 and ABT-199) compared to mice treated with the Vehicle or with LY3410738 alone. Significant reduction of spleen weight induced with ABT-199, but so significant difference between ABT-199 alone or in combination with LY3410738. (Figure 44).

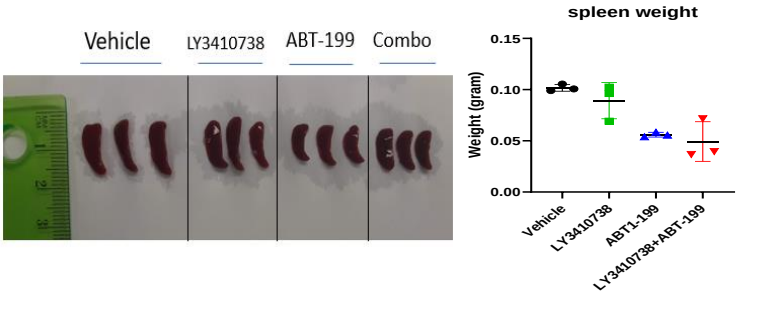

Figure 44: Spleen size and weight of PD study of PDX #2 in the combination therapy

Counting the viable cells collected from the spleen and BM with trypan blue revealed decrease in the number of the cells and the number of the hCD45, after magnetic sorting, from the spleen of the mice treated with the combination therapy, however no significant difference was detected in the cells counted from BM (Figure 45).

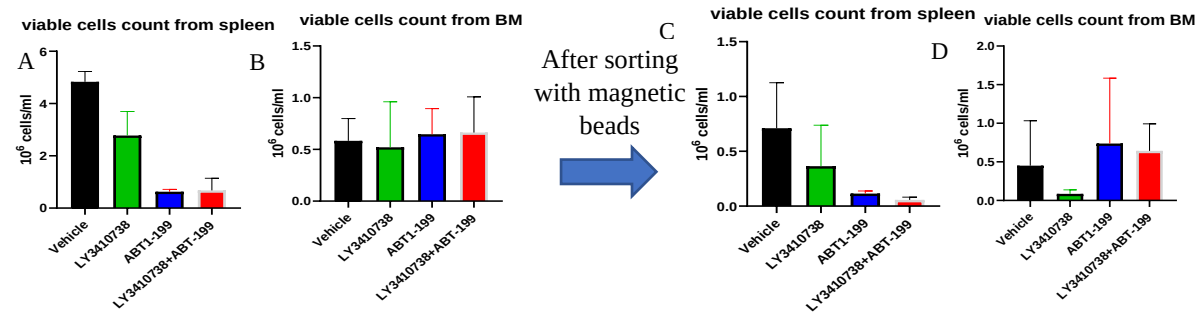

Figure 45: Spleen and BM cells counting before and after sorting with magnetic beads, PD study of PDX #2 of the combination study.

A.Spleens cell count before sorting. B. BM cell count before sorting. C. Spleens cell count after sorting. D. BM cell count after sorting.

Flowcytometry:

Flowcytometry analysis of cells which were collected from blood, spleen and BM was done. Further decrease in AML tumor burden (detected by the percentage of hCD33+/hCD45+ cells) was detected in the PB, spleen and BM in the mice treated with the ABT-199 and the combination therapy compared to LY3410738 alone (Figure 46). Percentage of hCD117+ cells, decreased in PB in LY3410738, ABT-199 and in the combination groups. While in spleen and BM; it decreased in the ABT-199 and the combination therapy groups. (Figure 47).

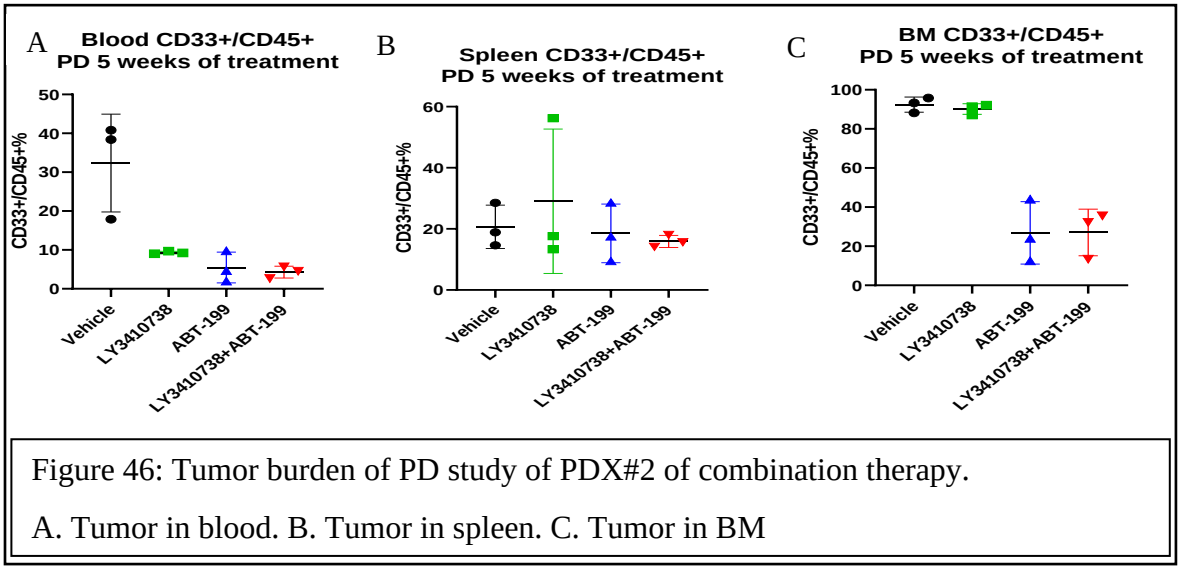

Figure 46: Tumor burden of PD study of PDX#2 of combination therapy.
A. Tumor in blood. B. Tumor in spleen. C. Tumor in BM

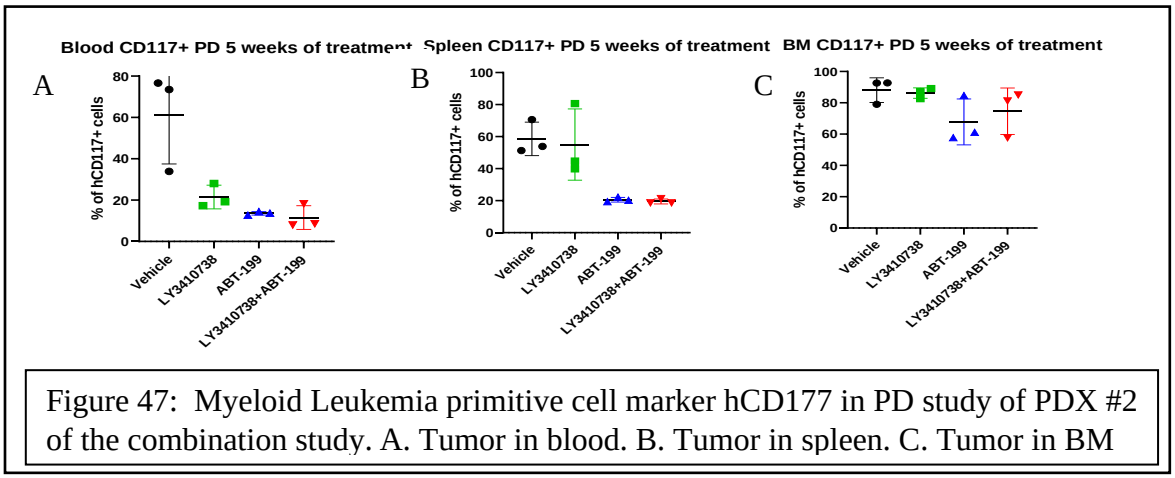

Figure 47: Myeloid Leukemia primitive cell marker hCD177 in PD study of PDX #2 of the combination study. A. Tumor in blood. B. Tumor in spleen. C. Tumor in BM

Increase in the differentiated populations (increase in the percentage of hCD15 (Figure 48 A) and hCD14 (Figure 48 B)) was detected in the mice treated with the LY3410738, while no significant increase in the differentiation markers in the Combination of ABT-199 groups compared with LY3410738, either in blood, spleen or BM.

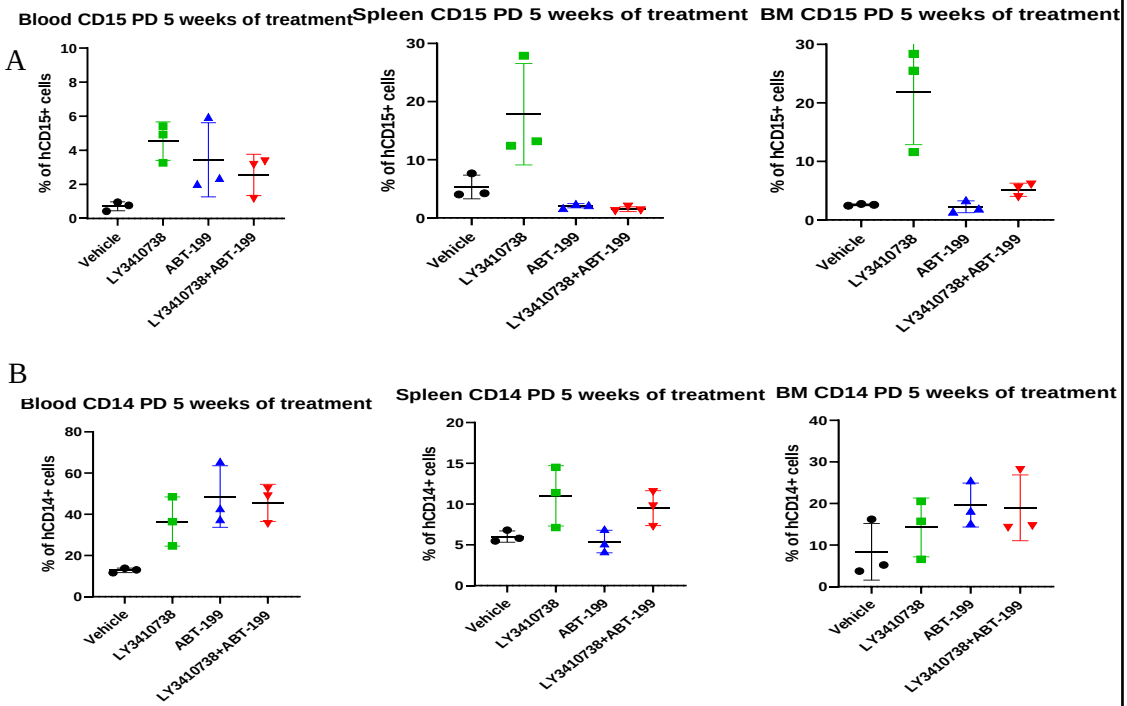

Figure 48: Differentiation markers in PD study of PDX#2 of the combination therapy study. A. CD15 marker. B. CD14 marker.

Hematoxylin and Eosin staining (H&E staining):

Femur bones of the sacrificed mice were saved in 10% formalin for H&E staining of the Bone Marrow. H&E staining revealed high tumor burden in the vehicle mice, as the whole BM is almost replaced with the blast cells (Figure 49 A). LY3410738 treated mice, the BM revealed high tumor burden with differentiation of the blast cells (Figure 49 B). ABT-199 treated mice, the BM is almost clear from the blast cells and showed a very low tumor burden (Figure 49 C). Mice treated with combination therapy, the BM showed low tumor burden compared with either Vehicle or LY3410738 alone, however no significant difference was detected between the BM of mice treated with the combination therapy or ABT-199 alone (Figure 49 D).

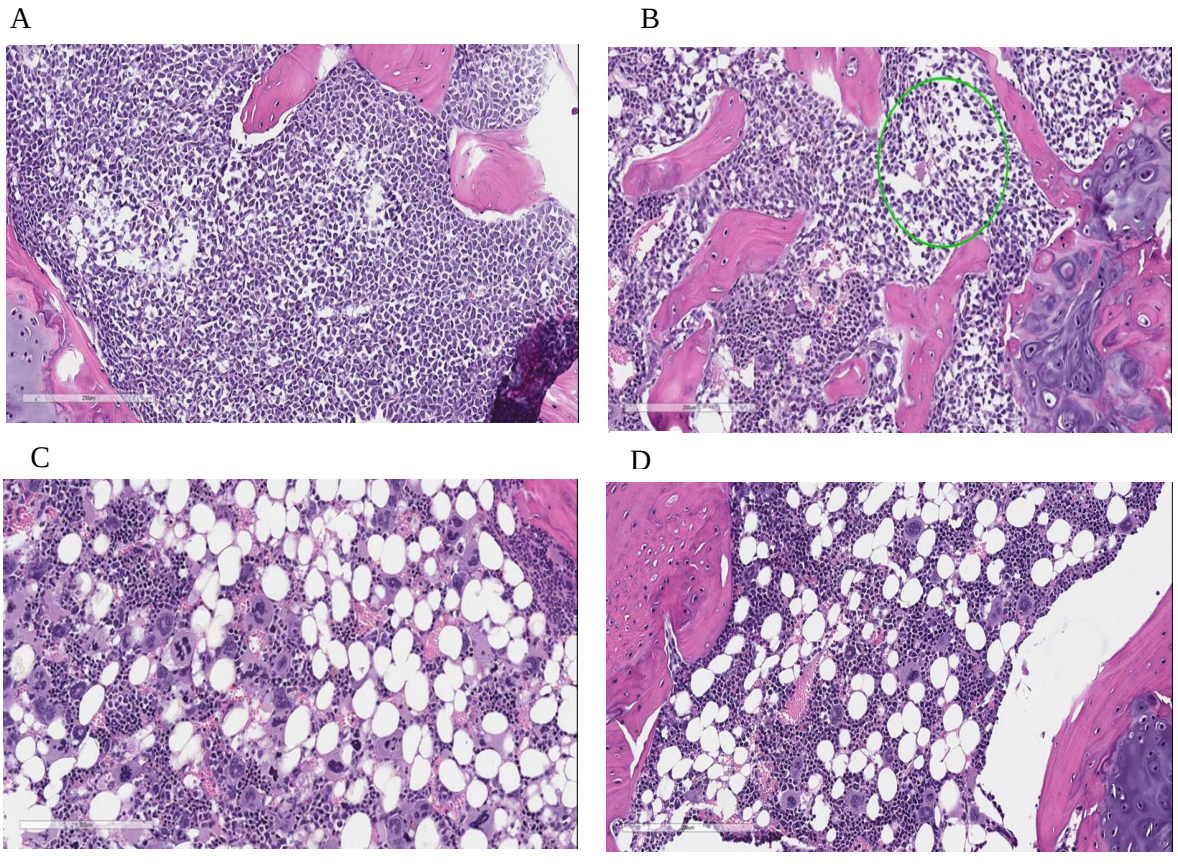

Figure 49: H&E staining of the BM of the PD study of PDX #2. A. Vehicle treated mice BM. B. LY3410738 treated mice BM. C. ABT-199 treated mice BM.

Aim 3-b. In Vitro: combination effect will be tested in the engineered MOLM14/R132 cell line and THP1/R132 cell line.

Additive reduction of viability with the combination therapy in MOLM14/R132 cell line after 8 days of sequential treatment but not after four days of treatment.

We induced the MOLM14/R132 cell line with Doxycycline for 4 days as planned and then different doses (0, 62.5, 125, 250, 500 or 1000nM) of LY3410738, ABT-199 or combined were added (Using 96 wells plates) and then we tested the combination efficacy using the CellTiter-Glo® Luminescent Cell Viability Assay (CTG Assay). Studying the combination efficacy after treatment for 4 days revealed that addition of ABT-199 to LY3410738 caused decrease in the viability of the cells after four days but no significant difference compared to ABT-199 alone in MOLM14/R132 cell lines (Figure 50).

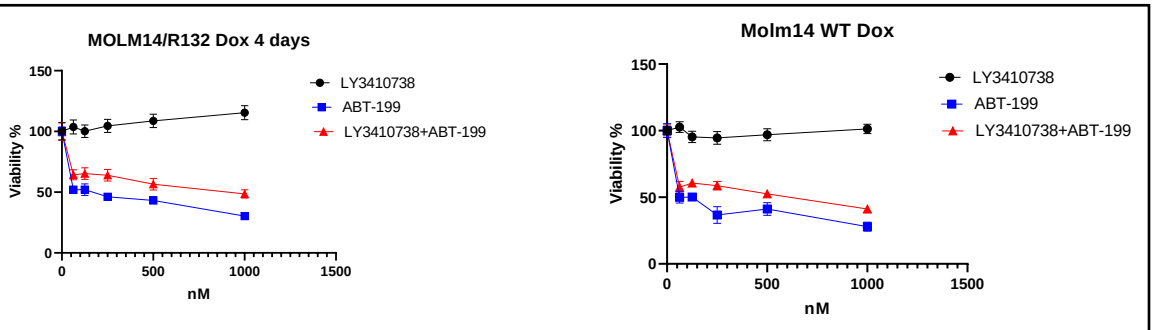

Figure 50: CTG Assay of the combination therapy in MOLM14 after 4 days.

We tested the combination therapy for a longer time and with smaller doses of ABT-199, in a sequential manner. Engineered MOLM14/R132 cell line was induced with 2µg/ml Doxycycline for 4 days, in a 24 well plates, we seeded 10,000 cells/ well in 1 ml of media with Doxycycline, then cells were treated with different doses of LY3410738 (0, 125, 250, 500 and 1000 nM) for 6 days (1x of drug was added in 0.5 every 2-3 days with doxycycline induction).

Different doses of ABT-199 (0, 25, 50, 100 and 200 nM) were added at day 6 for 2 days, cells were collected to measure the viability. The anti-leukemia efficacy was examined by Trypan Blue, Annexin V/DAPI and CTG assays. Addition of ABT-199 caused additive reduction of the viability (detected either with trypan blue, CTG assay or flowcytometry with Annexin V/DAPI assay (% of Annexin V-/DAPI- cells)) (Figure 51) and increase in the apoptosis (detected with increase in percentage of the Annexin V+ and Annexin V+/DAPI+) in MOLM14/R132 cell line (Figure 52).

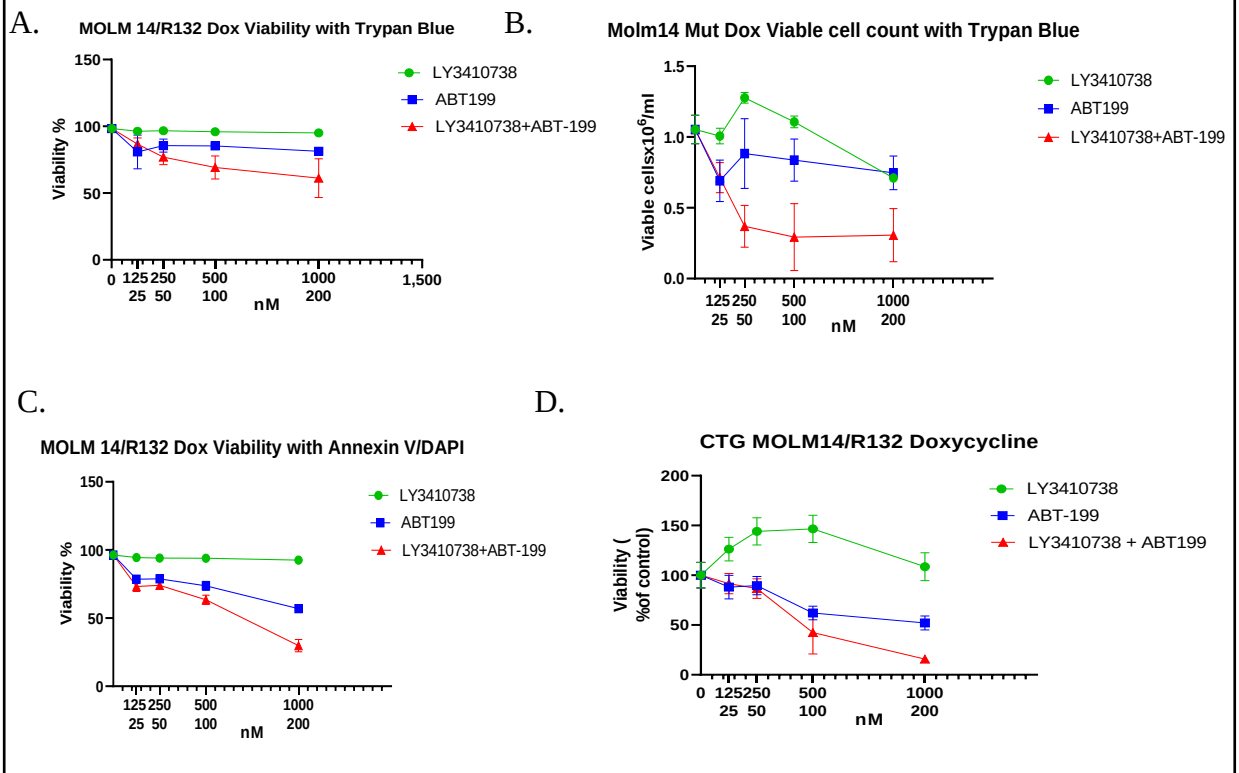

Figure 51: The anti-leukemic efficacy of the combination therapy in engineered MOLM14/R132 cell line.

A. Reduction of % of viability was detected in the combination therapy using trypan blue. B. Counting the viable cells using trypan blue, revealed reduction of the viable cells in the combination therapy compared with single agents. C. Additive reduction of the viability (% of Annexin V-/DAPI- cells) was detected with Annexin V/DAPI assay using flowcytometry. D. additive reduction of the viability (% of metabolically active cells) was detected with CTG Assay.

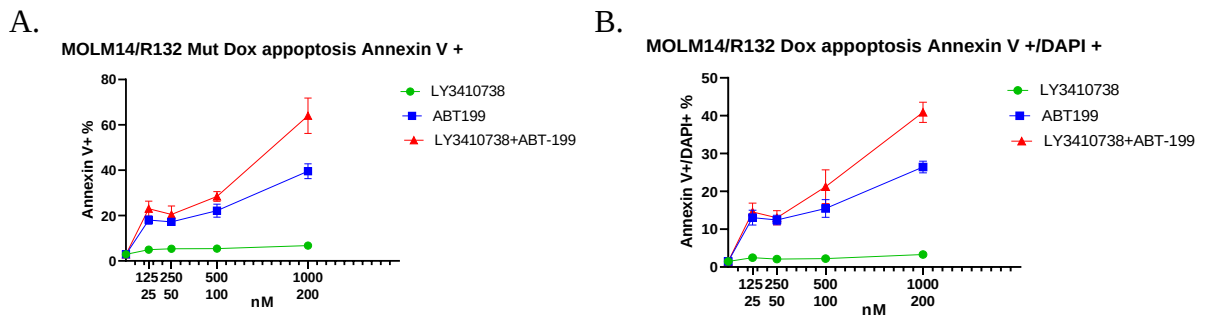

Figure 52: Studying the effect of the combination therapy (LY3410738 + ABT-199) on the apoptosis in engineered MOLM14/R132 cell line. A. Additive increase in the early apoptosis with the combination therapy was detected by increase the percentage of Annexin V + cells compared with each drug alone using flowcytometry. B. Additive increase in the late apoptosis in the combination therapy was detected by increase in the percentage of Annexin V+/DAPI + cells using flowcytometry.

No Additive reduction of viability with the combination therapy in THP1/R132 cell line either after 4 days of treatment or after 8 days of sequential treatment.

We induced the THP1/R132 cell line with Doxycycline for 4 days and then different doses of LY3410738, ABT-199 or combined were added (Using 96 wells plates). We tested the combination efficacy using the CTG Assay. Studying the combination efficacy after treatment revealed that addition of ABT-199 to LY3410738 caused decrease in the viability of the cells after four days but no significant difference was detected compared to ABT-199 alone in THP1/R132 cell lines (Figure 53).

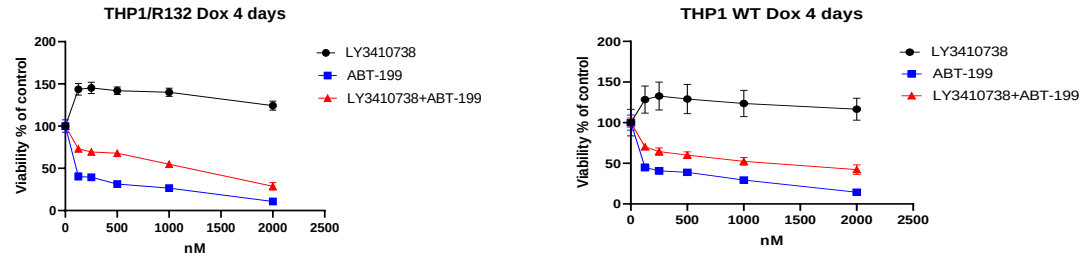

Figure 53: CTG Assay of the combination therapy in THP1 after 4 days.

Examining the combination therapy for a longer time and with smaller doses of ABT-199, in a sequential manner in engineered THP1/R132 cell line didn't show any significant difference in the viability tested with either trypan blue or Annexin V/DAPI assay. THP1/R132 cell line was induced with 2µg/ml Doxycycline for 4 days, in a 24 well plates we cultured 50,000 cells/ well in 1 ml of media with Doxycycline, then cells were treated with different doses of LY3410738 (0. 125, 250, 500 and 1000 nM) for 5 days (1x of drug was added in 0.5 every 2 days with doxycycline added). Different doses of ABT-199 (0, 25, 50, 100 and 200 nM) were added at day 5 for 2 days, then cells were collected to measure the viability. The anti-leukemia efficacy was examined by Trypan Blue, Annexin V/DAPI assay. Addition of ABT-199 didn't show any additive reduction of the viability (detected either with trypan blue (Figure 54A) or flowcytometry with Annexin V/DAPI Assay (Figure 54B)). No increase in the apoptosis (the percentage of the Annexin V+ (Figure 54C) and Annexin V+/DAPI+ (Figure 54D.)) was detected in THP1/R132 cell line.

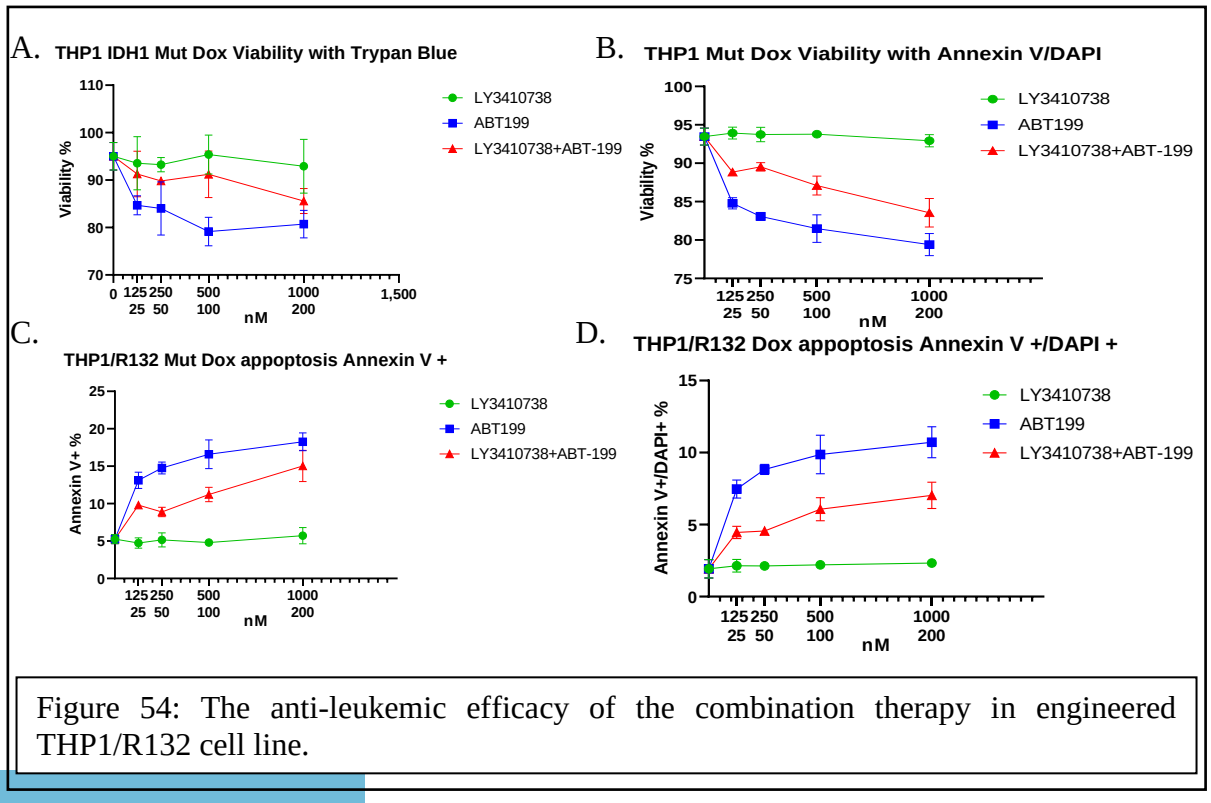

Figure 54: The anti-leukemic efficacy of the combination therapy in engineered THP1/R132 cell line.

Discussion:

Isocitrate dehydrogenase 1 gene mutations were identified in AML samples (6). Several studies proved that these mutations are acquired in the early steps of leukemia progression from hematopoietic stem cells (HSCs) (23, 24), and they are recurrent and have an important role in blocking the myeloid cells differentiation and progression of AML. Dual studies of diagnosis and relapse samples demonstrated that IDH1 mutations are stable during AML evolution either during the diagnosis or after relapse (25), indicating that some subclones harbor IDH1 mutation are able to survive during and after chemotherapy and contribute to relapse. These findings provide a strong need for new targeted therapies of mutated IDH1 enzyme, to selectively inhibit that enzyme and reduce the rate of adverse effects developed from the regular chemotherapy. The discovery of AG-120 (ivosidenib) presented a novel class of cancer therapy as an allosteric inhibitor of mIDH1, dependent on induction of cellular differentiation and maturation of myeloid blasts (14). However, recent studies showed some patients are refractory or resistant to AG120 (26). This raises the need for development of more potent inhibitors targeting IDH1.

Recently, a big number of covalent inhibitors has been developed for human enzymes. Several of these covalent inhibitors have already been approved by FDA for use in human patients, due to high potency, durability and irreversibly inhibiting the targeted enzymes. Eli Lilly and Company has developed a novel potent covalent mIDH1 inhibitor, and as a covalent inhibitor we hypothesized that it will act faster and more durably than the reversible mIDH1 inhibitor; AG120.

In our preclinical studies we proved that LY3410738 faster and durably inhibited mIDH1 enzyme in engineered AML cells with mIDH1 *in vitro*, detected with rapid reduction of media

2-HG levels after treatment with smaller dose of LY3410738, compared with AG120. In our study we used 0.1μM as a smaller dose in engineered cell line and (0, 0.012, 0.037, 0.111, 0.333) doses in testing the efficacy in primary AML sample, while in AG120 study, they tested 0.5μM as the smallest dose (14). We found limitations in studying the induction of differentiation *in vitro* in the engineered cell lines with flow cytometry, however, we used the PMA Differentiation Assay that is tested before to induce the THP1 cell line into macrophages (17, 27). IDH1 mutation blocked differentiation and addition of LY3410738 could release that block and induce cellular differentiation significantly more that AG120, detected with the counting the differentiated attached cell. Furthermore, LY3410738 induced blast cellular differentiation in primary AML sample with mIDH1, refractory to AG120, however we couldn't detect significant differentiation in another two patient samples.

Interestingly, *in vivo* LY3410738 could decrease the levels of 2-HG in plasma collected from mice earlier and deeper than AG120 in AML PDX model refractory to AG120. Additionally, it induces differentiation detected with increase in the percentage of hCD15+ and hCD14+ cells. LY3410738 could significantly decrease the tumor burden detected with hCD33+/hCD45+ cells, however has no effect on the survival rate. Aggressiveness of the disease was a big limitation in our study as mice died rapidly without following the significant effect on the tumor burden and the survival, as IDH1 inhibitor, our novel drug, requires long time to detect the induction of differentiation and cell death. FLT3 mutations, are the most common mutations detected in AML patient samples according to TCGA data. Most of AML patients with IDH1 mutation develop FLT3 mutation which increase the progression and aggressiveness of the disease. Hardly we could find PDX models with IDH1 mutation without

FLT3 mutations which increase the aggressiveness of the leukemia and develop resistance to IDH1 inhibitors, furthermore, most of mIDH1 patient samples without FLT3 failed to engraft.

To further evaluate the molecular mechanism of action of the novel mIDH1inhibitor through gene enrichment analyses, RNAseq of human leukocytes collected from mice spleen demonstrated that LY3410738 induced IL1RL1, Lysozyme, PLD1, CCL5 and Cathepsin G genes upregulation which play a major rule in induction of myeloid cells differentiation and activation. Previous studies of identifying the genes regulated and downregulated by IDH1 mutation in glioma demonstrated that IDH1 mutation induced downregulation of the interleukins and chemokines (28), and interestingly we demonstrated that our IDH inhibitor could upregulate the cytokines and chemokines. Induction of cytokines and chemokines release and binding caused by LY3410738, most probably is a strong sign of differentiation, it also could be the reason of the differentiation syndrome which is the most common adverse effect of the drugs inducing differentiation as reported from ATRA therapy (29).

Multiple studies proved that IDH1 mutations induced global DNA hypermethylation mainly in the promotor site, these epigenetic modifications are the cause of block of myeloid cells differentiation and formation of myeloid leukemia, and use of IDH1 inhibitors reverse that DNA hypermethylation and release the block of differentiation and cause cell death, (9, 12, 30, 31). However, in our study we couldn't detect a significant effect of the IDH1 inhibitor on the global DNA methylation, changing the time point could has a great effect, but our mice quickly died due to the aggressiveness of the disease. Interestingly, we found some hypomethylated genes induced with LY3410738 were also upregulated detected in RNAseq analysis, these genes have an important role in induction of differentiation.

Recent preclinical studies confirmed the efficacy of selective BCL2 inhibitor (ABT-199) in the treatment of AML either *in vivo* or *in vitro*, even with smaller doses used, ABT-199 was very effective in induction of apoptosis and AML cells death (32). Additionally, it is proved that IDH1 mutations in AML increase the sensitivity to ABT-199 through inhibition of COX mediated by accumulation of 2-HG in IDH1 mutant AML cells and, consequently, increases the dependency on BCL-2 to prevent apoptosis (16). Preclinical studies also proved that combination therapy with IDH2 inhibitor and ABT-199 is a promising therapeutic approach for IDH2-mutated AML which support the ongoing clinical trials of the combination therapy of IDH inhibitor and ABT-199 (Venetoclax) (33).

Accordingly, here we tested the efficacy of the combination of the novel IDH1 inhibitor with ABT-199 in PDX models and in engineered cell lines, and we demonstrated increase efficacy of the antileukemic effect of the IDH1 inhibitor after addition of the selective BCL2 inhibitor (ABT-199), but no significant difference was detected between the combination therapy and ABT-199 as a single agent till six weeks of treatment *in vivo*. Since LY3410738 needs extra time to show the efficacy on the tumor burden after robust of induction of differentiation, we expect that using less aggressive PDX models with longer survival, will facilitate the synergistic effect of the combination therapy. *In vitro* studies using Engineered MOLM14/R132 cell line, demonstrated increase the antileukemic efficacy of the combination therapy compared with each drug alone, sequential treatment for eight days revealed the increase of the antileukemic efficacy of the combination therapy, however we need to test the efficacy of the combination therapy in more samples *in vitro* either other cell lines or patients samples. .

In our data we noticed increase in the cytokines and chemokines binding with the novel covalent IDH1 inhibitor; LY3410738. Studies indicated that cytokines promote cellular survival through induction of BCL2 after activation of different pathways as STAT, PI3K or MAPK (34, 35). These findings support our rational combination of LY3410738, further mechanistic investigations of different pathways are needed to validate our hypothesis.

LY3410738 will represent the first in class as a covalent allosteric inhibitor of the mutant IDH1 used in the treatment of AML. The potency of the novel covalent IDH1 inhibitor shown in our study compared with the FDA approved AG120 will be an important reason to be used in the new clinical trials in the treatment of chemotherapy relapsed AML patients with mutant IDH1. It also will open new fields of a targeted therapy to inhibit other mutant IDH1 tumors such as gliomas. In addition, the response rate to single IDH1 inhibitor in relapsed AML is low (in the range of 40%), that increase the need to the combination therapy. Our studies of the combination of the novel IDH1 inhibitor with ABT-199 will open new horizons in the treatment of AML. Furthermore, testing the combination of the novel IDH1 inhibitor with other targeted therapies such as FLT3 inhibitors or hypomethylating agent.

Conclusion:

Collectively, our cumulative preclinical data collected in this study supports that LY3410738 represents the first potent covalent IDH1 inhibitor in Acute Myeloid Leukemia with IDH1/R132 mutation. It decreases 2-HG levels earlier than Ivosedineb (AG120) and induces release the block of differentiation with respect to AG120, but it does not have much effect in the survival rate. LY3410738 induced reduction of 2-HG and induction of differentiation in AML samples refractory to AG120 *in vitro* and *in vivo*. Interestingly, we noticed that the novel covalent IDH1 inhibitor; LY3410738 has a strong role in induction of the immune response and increase in the inflammatory mediators compared with AG120. It exhibits enhanced efficacy in combination with Venetoclax. Addition of ABT-199 enhanced reduction of tumor burden and facilitation of more differentiation, however, no significant difference between the combination therapy and ABT-199 as a single agent was detected. This combination therapy may open new horizons of the new combination therapies with IDH1 inhibitors in the treatment of AML.

Future Directions:

Beyond testing the efficacy of the combination therapy of LY3410738 we need to further study the rational mechanism of action of combining the LY3410738 with ABT-199 by evaluating the effect of the novel LY3410738 on the BCL2 protein level and assisting the participation of different pathways which may be activated or upregulated with the increase in the cytokines and chemokines binding induced with LY3410738 treatment. We are also planning to study the effect of the upregulated genes detected with RNA sequencing on the protein levels and validate the effect of theses genes changes on the proteins responsible for

activation of different pathways that play rules in induction of differentiation, promoting of cell death and affecting the immune response.

Furthermore, as long as most of AML PDX models with IDH1 mutation are accompanied by FLT3 mutations which induce the aggressiveness of the disease and increase the rate of resistance to IDH1 inhibitors, we intend to examine the efficacy of the novel IDH1 inhibitor LY3410738 in AML PDX models with mIDH1 but without FLT3 mutation or use engineered mice models without FLT3 mutation.

To evaluate the efficacy of the novel LY3410738 compared with AG120, we need to address the mechanisms of resistance to AG120 treatment and examine the efficacy of LY3410738 in the known PDX models resistant to AG120.

To expand our knowledge about the rational efficacy of the novel IDH1 inhibitor, we have to test the rationale combinations of novel IDH1 inhibitor with other targeted agents as DNA hypomethylating agents, or FLT3 inhibitors.

Biblography:

1. Rieger MA, Schroeder T. Hematopoiesis. Cold Spring Harb Perspect Biol. 2012;4(12).

2. Dohner H, Weisdorf DJ, Bloomfield CD. Acute Myeloid Leukemia. N Engl J Med. 2015;373(12):1136-52.

3. Clark O, Yen K, Mellinghoff IK. Molecular Pathways: Isocitrate Dehydrogenase Mutations in Cancer. Clin Cancer Res. 2016;22(8):1837-42.

4. Molenaar RJ, Radivoyevitch T, Maciejewski JP, van Noorden CJ, Bleeker FE. The driver and passenger effects of isocitrate dehydrogenase 1 and 2 mutations in oncogenesis and survival prolongation. Biochim Biophys Acta. 2014;1846(2):326-41.

5. Parsons, D. W, Jones, S, Zhang, X, Lin, J. C, Leary, R. J, Angenendt, P, Mankoo, P, arter, H, Siu, I. M, Gallia, G. L, Olivi, A, McLendon, R, Rasheed, B. A, Keir, S, Nikolskaya, T, Nikolsky, Y, Busam, D. A, Tekleab, H, Diaz, L. A. Jr, Hartigan, J, Smith, D. R, Strausberg, R. L, Marie, S. K, Shinjo, S. M, Yan, H, Riggins, G. J, Bigner, D. D, Karchin, R, Papadopoulos, N, Parmigiani, G, Vogelstein, B, Velculescu, V. E, Kinzler, K. W. An integrated genomic analysis of human glioblastoma multiforme. Science. 2008;321(5897):1807-12.

6. Mardis, E. R, Ding, L, Dooling, D. J, Larson, D. E, McLellan, M. D, Chen, K, Koboldt, D. C, Fulton, R. S, Delehaunty, K. D, McGrath, S. D, Fulton, L. A, Locke, D. P, Magrini, V. J, Abbott, R. M, Vickery, T. L, Reed, J. S, Robinson, J. S, Wylie, T, Smith, S. M, Carmichael, L, Eldred, J. M, Harris, C. C, Walker, J, Peck, J. B, Du, F, Dukes, A. F, Sanderson, G. E, Brummett, A. M, Clark, E, McMichael, J. F, Meyer, R. J, Schindler, J. K, Pohl, C. S, Wallis, J. W, Shi, X, Lin, L, Schmidt, H, Tang, Y, Haipek, C, Wiechert, M. E, Ivy, J. V, Kalicki, J. Elliott, G, Ries, R. E, Payton, J. E, Westervelt, P, Tomasson, M. H, Watson, M. A, Baty, J.

Heath, S, Shannon, W. D, Nagarajan, R, Link, D. C, Walter, M. J, Graubert, T. A, DiPersio, J. F, Wilson, R. K, Ley, T. J. Recurring mutations found by sequencing an acute myeloid leukemia genome. N Engl J Med. 2009;361(11):1058-66.

7. Marcucci, G, Maharry, K, Wu, Y. Z, Radmacher, M. D, Mrozek, K, Margeson, D, Holland, K. B, Whitman, S. P, Becker, H, Schwind, S, Metzeler, K. H, Powell, B. L, Carter, T. H, Kolitz, J. E, Wetzler, M, Carroll, A. J, Baer, M. R, Caligiuri, M. A, Larson, R. A, Bloomfield, C. D. IDH1 and IDH2 gene mutations identify novel molecular subsets within de novo cytogenetically normal acute myeloid leukemia: a Cancer and Leukemia Group B study. J Clin Oncol. 2010;28(14):2348-55.

8. Dang, L, White, D. W, Gross, S, Bennett, B. D, Bittinger, M. A, Driggers, E. M, Fantin, V. R, Jang, H. G, Jin, S, Keenan, M. C, Marks, K. M, Prins, R. M, Ward, P. S, Yen, K. E, Liau, L. M, Rabinowitz, J. D, Cantley, L. C, Thompson, C. B, Vander Heiden, M. G, Su, S. M. Cancer-associated IDH1 mutations produce 2-hydroxyglutarate. Nature. 2010;465(7300):966.

9. Sasaki, M, Knobbe, C. B, Munger, J. C, Lind, E. F, Brenner, D, Brustle, A, Harris, I. S, Holmes, R, Wakeham, A, Haight, J, You-Ten, A, Li, W. Y, Schalm, S, Su, S. M, Virtanen, C, Reifenberger, G, Ohashi, P. S, Barber, D. L, Figueroa, M. E, Melnick, A, Zuniga-Pflucker, J. C, Mak, T. W. IDH1(R132H) mutation increases murine haematopoietic progenitors and alters epigenetics. Nature. 2012;488(7413):656-9.

10. Koszarska, M, Bors, A, Feczko, A, Meggyesi, N, Batai, A, Csomor, J, Adam, E, Kozma, A, Orban, T. I, Lovas, N, Sipos, A, Karaszi, E, Dolgos, J, Fekete, S, Reichardt, J, Lehoczky, E, Masszi, T, Tordai, A, Andrikovics, H. Type and location of isocitrate dehydrogenase mutations influence clinical characteristics and disease outcome of acute myeloid leukemia. Leuk Lymphoma. 2013;54(5):1028-35.

11. Boissel, N, Nibourel, O, Renneville, A, Gardin, C, Reman, O, Contentin, N, Bordessoule, D, Pautas, C, de Revel, T, Quesnel, B, Huchette, P, Philippe, N, Geffroy, S, Terre, C, Thomas, X, Castaigne, S, Dombret, H, Preudhomme, C. Prognostic impact of isocitrate dehydrogenase enzyme isoforms 1 and 2 mutations in acute myeloid leukemia: a study by the Acute Leukemia French Association group. J Clin Oncol. 2010;28(23):3717-23.

12. Figueroa, M. E, Abdel-Wahab, O, Lu, C, Ward, P. S, Patel, J, Shih, A, Li, Y, Bhagwat, N, Vasanthakumar, A, Fernandez, H. F, Tallman, M. S, Sun, Z, Wolniak, K, Peeters, J. K, Liu, W, Choe, S. E, Fantin, V. R, Paietta, E, Lowenberg, B, Licht, J. D, Godley, L. A, Delwel, R, Valk, P. J, Thompson, C. B, Levine, R. L, Melnick, A. Leukemic IDH1 and IDH2 mutations result in a hypermethylation phenotype, disrupt TET2 function, and impair hematopoietic differentiation. Cancer Cell. 2010;18(6):553-67.

13. DiNardo CD, Patel KP, Garcia-Manero G, Luthra R, Pierce S, Borthakur G, e, Jabbour, E, Kadia, T, Pemmaraju, N, Konopleva, M, Faderl, S, Cortes, J, Kantarjian, H. M, Ravandi, F. Lack of association of IDH1, IDH2 and DNMT3A mutations with outcome in older patients with acute myeloid leukemia treated with hypomethylating agents. Leuk Lymphoma. 2014;55(8):1925-9.

14. Popovici-Muller J, Lemieux RM, Artin E, Saunders JO, Salituro FG, Travins J, Cianchetta, G, Cai, Z, Zhou, D, Cui, D, Chen, P, Straley, K, Tobin, E, Wang, F, David, M. D, Penard-Lacronique, V, Quivoron, C, Saada, V, de Botton, S, Gross, S, Dang, L, Yang, H, Utley, L, Chen, Y, Kim, H, Jin, S, Gu, Z, Yao, G, Luo, Z, Lv, X, Fang, C, Yan, L, Olaharski, A, Silverman, L, Biller, S, Su, S. M, Yen, K. Discovery of AG-120 (Ivosidenib): A First-in-Class Mutant IDH1 Inhibitor for the Treatment of IDH1 Mutant Cancers. ACS Med Chem Lett. 2018;9(4):300-5.

15. Roberts AW, Huang D. Targeting BCL2 With BH3 Mimetics: Basic Science and Clinical Application of Venetoclax in Chronic Lymphocytic Leukemia and Related B Cell Malignancies. Clin Pharmacol Ther. 2017;101(1):89-98.

16. Chan SM, Thomas D, Corces-Zimmerman MR, Xavy S, Rastogi S, Hong WJ, Zhao, F, Medeiros, B. C, Tyvoll, D. A, Majeti, R. Isocitrate dehydrogenase 1 and 2 mutations induce BCL-2 dependence in acute myeloid leukemia. Nat Med. 2015;21(2):178-84.

17. Urban DJ, Martinez NJ, Davis MI, Brimacombe KR, Cheff DM, Lee TD, Henderson, M. J, Titus, S. A, Pragani, R, Rohde, J. M, Liu, L, Fang, Y, Karavadhi, S, Shah, P, Lee, O. W, Wang, A, McIver, A, Zheng, H, Wang, X, Xu, X, Jadhav, A, Simeonov, A, Shen, M, Boxer, M. B, Hall, M. D. Assessing inhibitors of mutant isocitrate dehydrogenase using a suite of pre-clinical discovery assays. Sci Rep. 2017;7(1):12758.

18. Catovsky D, de Salvo Cardullo L, O'Brien M, Morilla R, Costello C, Galton D, Ganeshaguru, K, Hoffbrand, V. Cytochemical markers of differentiation in acute leukemia. Cancer Res. 1981;41(11 Pt 2):4824-32.

19. Bechoua S, Daniel LW. Phospholipase D is required in the signaling pathway leading to p38 MAPK activation in neutrophil-like HL-60 cells, stimulated by N-formyl-methionyl-leucyl-phenylalanine. J Biol Chem. 2001;276(34):31752-9.

20. Zhang M, Sukhumalchandra P, Enyenihi AA, St John LS, Hunsucker SA, Mittendorf EA, Sergeeva, A, Ruisaard, K, Al-Atrache, Z, Ropp, P. A, Jakher, H, Rodriguez-Cruz, T, Lizee, G, Clise-Dwyer, K, Lu, S, Molldrem, J. J, Glish, G. L, Armistead, P. M, Alatrash, G. A novel HLA-A*0201 restricted peptide derived from cathepsin G is an effective immunotherapeutic target in acute myeloid leukemia. Clin Cancer Res. 2013;19(1):247-57.

21. Gomes-Silva D, Atilla E, Atilla PA, Mo F, Tashiro H, Srinivasan M, Lulla, P, Rouce, R. H, Cabral, J. M. S, Ramos, C. A, Brenner, M. K, Mamonkin, M. CD7 CAR T Cells for the Therapy of Acute Myeloid Leukemia. Mol Ther. 2019;27(1):272-80.

22. Zhang TJ, Zhou JD, Zhang W, Lin J, Ma JC, Wen XM, Yuan, Q, Li, X. X, Xu, Z. J, Qian, J. H19 overexpression promotes leukemogenesis and predicts unfavorable prognosis in acute myeloid leukemia. Clin Epigenetics. 2018;10:47.

23. Shlush LI, Zandi S, Mitchell A, Chen WC, Brandwein JM, Gupta V, Kennedy, J. A, Schimmer, A. D, Schuh, A. C, Yee, K. W, McLeod, J. L, Doedens, M, Medeiros, J. J, Marke, R, Kim, H. J, Lee, K, McPherson, J. D, Hudson, T. J, Brown, A. M, Yousif, F, Trinh, Q. M, Stein, L. D, Minden, M. D, Wang, J. C, Dick, J. E. Identification of pre-leukaemic haematopoietic stem cells in acute leukaemia. Nature. 2014;506(7488):328-33.

24. Chan SM, Majeti R. Role of DNMT3A, TET2, and IDH1/2 mutations in pre-leukemic stem cells in acute myeloid leukemia. Int J Hematol. 2013;98(6):648-57.

25. Chou WC, Hou HA, Chen CY, Tang JL, Yao M, Tsay W, Ko, B. S, Wu, S. J, Huang, S. Y, Hsu, S. C, Chen, Y. C, Huang, Y. N, Chang, Y. C, Lee, F. Y, Liu, M. C, Liu, C. W, Tseng, M. H, Huang, C. F, Tien, H. F. Distinct clinical and biologic characteristics in adult acute myeloid leukemia bearing the isocitrate dehydrogenase 1 mutation. Blood. 2010;115(14):2749-54.

26. DiNardo CD. Ivosidenib in IDH1-Mutated Acute Myeloid Leukemia. N Engl J Med. 2018;379(12):1186.

27. Gatto F, Cagliani R, Catelani T, Guarnieri D, Moglianetti M, Pompa PP, Bardi, G. PMA-Induced THP-1 Macrophage Differentiation is Not Impaired by Citrate-Coated Platinum Nanoparticles. Nanomaterials (Basel). 2017;7(10).

28. Ren J, Lou M, Shi J, Xue Y, Cui D. Identifying the genes regulated by IDH1 via gene-chip in glioma cell U87. Int J Clin Exp Med. 2015;8(10):18090-8.

29. Sanz MA, Montesinos P. How we prevent and treat differentiation syndrome in patients with acute promyelocytic leukemia. Blood. 2014;123(18):2777-82.

30. Wiehle L, Raddatz G, Pusch S, Gutekunst J, von Deimling A, Rodriguez-Paredes M, Lyko, F. mIDH-associated DNA hypermethylation in acute myeloid leukemia reflects differentiation blockage rather than inhibition of TET-mediated demethylation. Cell Stress. 2017;1(1):55-67.

31. Unruh D, Zewde M, Buss A, Drumm MR, Tran AN, Scholtens DM, Horbinski, C. Methylation and transcription patterns are distinct in IDH mutant gliomas compared to other IDH mutant cancers. Sci Rep. 2019;9(1):8946.

32. Pan R, Hogdal LJ, Benito JM, Bucci D, Han L, Borthakur G, Cortes, J, DeAngelo, D. J, Debose, L, Mu, H, Dohner, H, Gaidzik, V. I, Galinsky, I, Golfman, L. S, Haferlach, T, Harutyunyan, K. G, Hu, J, Leverson, J. D, Marcucci, G, Muschen, M, Newman, R, Park, E, Ruvolo, P. P, Ruvolo, V, Ryan, J, Schindela, S, Zweidler-McKay, P, Stone, R. M, Kantarjian, H, Andreeff, M, Konopleva, M, Letai, A. G. Selective BCL-2 inhibition by ABT-199 causes on-target cell death in acute myeloid leukemia. Cancer Discov. 2014;4(3):362-75.

33. Severine Cathelin P, David Sharon, PhD , Amit Subedi, PhD , Dan Cojocari, PhD BSc , Darren C. Phillips, PhD , Joel D. Leverson, PhD , Kyle MacBeth, PhD , Brandon Nicolay , Rohini Narayanaswamy , Sebastien Ronseaux , Guowen Liu, PhD , Steven M Chan, MD PhD. Combination of Enasidenib and Venetoclax Shows Superior Anti-Leukemic Activity Against IDH2 Mutated AML in Patient-Derived Xenograft Models. blood. 2018;132(Issue Supplement 1):562.

34. Aronica MA, Goenka S, Boothby M. IL-4-dependent induction of BCL-2 and BCL-X(L)IN activated T lymphocytes through a STAT6- and pi 3-kinase-independent pathway. Cytokine. 2000;12(6):578-87.

35. Moye PW, Blalock WL, Hoyle PE, Chang F, Franklin RA, Weinstein-Oppenheimer C, et al. Synergy between Raf and BCL2 in abrogating the cytokine dependency of hematopoietic cells. Leukemia. 2000;14(6):1060-79.

Vita

Vivian Fawzy Awad Salama was born in Alexandria, Egypt. The daughter of Fawzy and Laila Salama. After completing her degree at Alraml High School, Alexandria, Egypt, in 2001, she was admitted to the Faculty of Medicine, University of Alexandria, Egypt. After six years, she graduated with Excellent with honor degree and then she started her internship at the Main Alexandria Hospitals, University of Alexandria, Egypt. Then she started her Residency in the internal medicine/ hematology department, at The Main Alexandria University Hospitals, University of Alexandria, Egypt. After moving to United States of America she joined the master of science program at the University of Texas, MD Anderson Cancer Center, UT Health Graduate School of Biomedical Sciences, Houston, Texas, USA, under the supervision of Dr. Marina Konopleva, MD, PHD.

Permanent address:

11502 Bay Ledge Dr.,

Pearland, Texas, USA. 77584